NASA TECHNICAL NOTE

NASA TN D-2590

NASA TN D-2590

DETERMINATION OF LOADS ON A FLEXIBLE LAUNCH VEHICLE DURING ASCENT THROUGH WINDS

by Harold C. Lester and Dennis F. Collins

Langley Research Center
Langley Station, Hampton, Va.

NATIONAL AERONAUTICS AND SPACE ADMINISTRATION • WASHINGTON, D. C. • FEBRUARY 1965

NASA TN D-2590

DETERMINATION OF LOADS ON A FLEXIBLE LAUNCH VEHICLE DURING ASCENT THROUGH WINDS

By Harold C. Lester and Dennis F. Collins

Langley Research Center
Langley Station, Hampton, Va.

NATIONAL AERONAUTICS AND SPACE ADMINISTRATION

For sale by the Office of Technical Services, Department of Commerce,
Washington, D.C. 20230 -- Price $3.00

CONTENTS

	Page
SUMMARY	1
INTRODUCTION	1
SYMBOLS	2
ANALYSIS	8
Mathematical Model	8
General	8
Bending modes	8
Propellant slosh	9
Method of Analysis	9
Lagrange's equations	9
Kinetic energy	10
Potential energy and dissipation function	13
Equations of Motion	14
Axial motion equation	15
Lateral motion equation	17
Pitch equation	17
Bending mode equation	18
Propellant slosh equation	19
Gimbaled engine equation	19
Control Equations	19
Feedback considerations	19
Gimbaled engine commands	20
Forces Acting on the Launch Vehicle	21
Propulsive forces	21
Aerodynamic forces	22
Wind inputs	23
COMPUTER PROGRAM	24
General	24
Propellant Slosh Considerations	25
Aerodynamic Considerations	25
Bending Moments	25
Integration Technique	26
Computing Interval Adjustment Criteria	26
APPLICATION AND RESULTS	27
Configuration	27
Mass and stiffness properties	27
Aerodynamics	27
Control system	27
Wind profile	28
Launch-Vehicle Response and Bending Loads	28
Trajectory	28

Page

Gimbaled engine, bending mode, and slosh responses 28
Bending moments 29

CONCLUDING REMARKS 29

APPENDIX A - SLENDER-BODY MOMENTUM AERODYNAMICS 31

APPENDIX B - QUASI-STEADY AERODYNAMICS 34

APPENDIX C - PROPULSIVE FORCES AND PROPELLANT FLOW EFFECTS 36

APPENDIX D - BENDING MOMENTS 41

APPENDIX E - SUMMARY OF EQUATIONS 44

REFERENCES 48

FIGURES 50

DETERMINATION OF LOADS ON A FLEXIBLE LAUNCH VEHICLE DURING ASCENT THROUGH WINDS

By Harold C. Lester and Dennis F. Collins
Langley Research Center

SUMMARY

An analytical procedure is developed for computing the pitch plane motions and bending moments experienced by a flexible launch vehicle during ascent through atmospheric winds. Structural bending is approximated by the superposition of several beam modes, and propellant slosh is treated by a mechanical analogy. Nonlinear, time-dependent equations of motion are derived by using a variational procedure which is applicable to variable mass systems. As an illustrative example, the method is applied to a typical launch vehicle and the responses computed numerically by means of an equivalent fifth-order integration. The method is particularly suitable for use with detailed wind velocity profiles such as those obtained by the smoke-trail technique.

INTRODUCTION

As a launch vehicle ascends through the atmosphere, it experiences disturbing influences from many sources, among which are winds, wind shears, and gusts. The loads resulting from the wind environment represent a major contribution to the total flight loads. Satisfactory structural design of a launch vehicle, therefore, requires that the system response to winds be fully understood in order to assure adequate structural integrity.

The prediction of launch-vehicle wind loads has usually been divided into two parts: (1) the rigid-body loads associated with winds and wind shears and (2) the flexible body loads resulting from response to gusts. With this approach, the rigid-body loads are determined by flying the rigid vehicle, described by equations with time-varying coefficients, through synthetic or measured wind profiles. Typical of such methods are the pitch plane analysis developed in reference 1 and the three-dimensional formulation, which includes wind directionality effects, presented in references 2 and 3. The synthetic wind profiles developed in reference 4 are examples of the inputs used in investigations of this type. Gust loads are estimated by analyzing the perturbation motion about discrete points in the boost trajectory. Fixed coefficient equations accounting for the structural flexibility degrees of freedom (for example, ref. 5) and gust inputs in the form of steps or sinusoids and ramps of different wavelengths are employed for this purpose. Design loads are determined by superposition of the rigid-body wind and wind-shear loads and gust loads. Although such an approach can be

justified on the basis of available measured wind data, improved wind-measurement techniques (ref. 6) indicate a need for a refined procedure.

In this paper, an analytical procedure is developed for computing the motions and bending moments experienced by a flexible launch vehicle during ascent through an atmospheric wind field. The procedure represents an extension of the methods previously discussed in that the effects of structural bending, time-dependent coefficients, and detailed wind inputs measured by the improved methods (ref. 6) and representing the combined influence of winds, wind shears, and gusts are considered jointly. Pitch plane motion is considered and referenced to a body-fixed Cartesian coordinate system. Structural bending is represented by the superposition of several free-free beam modes and a simple spring-mass analogy is used to approximate propellant slosh. Nonlinear equations of motion which have time-dependent coefficients are derived by using a variational procedure (ref. 7) which is applicable to variable mass systems. Both quasi-steady and slender-body momentum aerodynamic coefficients are derived. The nonlinear equations of motion are solved numerically on a digital computer by means of an equivalent fifth-order integration using a fourth-order Runge-Kutta routine.

The paper is divided into three major sections: Analysis, Computer Program, and Application and Results. In the section "Analysis" the governing equations are derived and the complete set of resulting equations are then summarized in an appendix. Salient features of the digital computer solution are discussed in the section "Computer Program." As reported in the section "Application and Results," the method is applied to a representative launch vehicle and the motions and bending moments computed for flight through a smoke-trail-derived wind velocity profile.

SYMBOLS

A_1, A_2 cross-sectional area of thrust chamber exit face, gimbaled and nongimbaled engines, respectively, sq ft

a_o control system gain

a_x assumed absolute axial acceleration time history, $\frac{T_e - qS_oC_A(M)}{m_t}$, ft/sec^2

$C_A(M)$ axial-force coefficient

$C_{N_\alpha}(M)$ slope of normal-force coefficient, $\int_0^L c_{n_\alpha}(x,M)\,dx$, radian^{-1}

C_b generalized bending-moment coefficient, used with appropriate subscript (see appendix D)

C_j	generalized aerodynamic coefficient associated with jth bending mode, used with appropriate subscript (see appendixes A and B)
C_m	generalized pitching-moment coefficient, used with appropriate subscript (see appendixes A and B)
$C_{m_\alpha}(M)$	slope of pitching-moment coefficient, $\int_0^L (x - x_{cg}) c_{n_\alpha}(x,M)\, dx$, ft/radian
C_n	generalized aerodynamic coefficient, used with appropriate subscript (see appendixes A and B)
$c_{n_\alpha}(x,M)$	slope of local normal-force coefficient, 1/ft-radian
D	dissipation function, ft-lb
d_1, d_2	distance from gimbal point to nozzle exit plane, gimbaled and nongimbaled engines, respectively, ft
E	total kinetic energy, ft-lb
$F_{a,x}$, $F_{a,y}$	component of aerodynamic force in x- and y-direction, respectively, lb
$F_{g,x}$, $F_{g,y}$	component of gravity force in x- and y-direction, respectively, lb
$F_{p,x}$, $F_{p,y}$	component of propulsive force in x- and y-direction, respectively, lb
F_x, F_y	component of arbitrary force in x- and y-direction, respectively, lb
g	gravitational acceleration constant, ft/sec^2
H,R	inertial axes (see fig. 1)
h,r	coordinates along inertial axes, denoting altitude and range, respectively, ft
I_{cg}	mass moment of inertia of launch vehicle (less engines) about center of gravity, lb-sec^2-ft
I_e, $I_{e,l}$	mass moment of inertia of all engines and gimbaled engine, respectively, about gimbal point, lb-sec^2-ft
i,j	modal indices
$\vec{i}, \vec{j}, \vec{k}$	unit vectors

K_c, K_f, K_o control system gains, sec, 1/sec, and 1/sec, respectively

k propellant slosh index

L length of launch vehicle, ft

$l(x,t)$, $l_I(x,t)$, $l_g(x,t)$ lateral aerodynamic, inertial, and gravitational loading, respectively, per unit length, lb/ft

M Mach number, $\frac{V_{m,w}}{V_s}$

$M_{a,cg}$ aerodynamic pitching moment about center of gravity, ft-lb

$M_{b,n}$ bending moment at station $x = x_{b,n}$, ft-lb

M_{cg} arbitrary pitching moment about center of gravity, ft-lb

M_p propulsive pitching moment about center of gravity, ft-lb

$m(x,t)$ launch-vehicle mass distribution per unit length, less engines, $\frac{\text{lb-sec}^2}{\text{sq ft}}$

$m(\eta_1), m(\eta_2)$ mass distribution per unit length, gimbaled and nongimbaled engines, respectively, $\frac{\text{lb-sec}^2}{\text{sq ft}}$

m_e, $m_{e,1}$ mass of all engines and gimbaled engine, respectively, $\frac{\text{lb-sec}^2}{\text{ft}}$

m_i generalized mass associated with ith bending mode, $\frac{\text{lb-sec}^2}{\text{ft}}$

m_k propellant slosh mass, $\frac{\text{lb-sec}^2}{\text{ft}}$

m_t total mass, launch vehicle plus engines, $\frac{\text{lb-sec}^2}{\text{ft}}$

$p_{e,1}$, $p_{e,2}$ exhaust pressure, gimbaled and nongimbaled engines, respectively, lb/ft^2

p_o atmospheric pressure at altitude h, lb/ft^2

$Q_{j,a}$ generalized aerodynamic force associated with jth bending mode, lb

$Q_{j,p}$ generalized propulsive force associated with jth bending mode, lb

$Q_{\beta i}$ generalized force associated with particular degree of freedom β_i

q dynamic pressure, $\frac{1}{2}\rho V_{m,w}^2$, lb/sq ft

$q_i(t)$ generalized coordinate associated with ith bending mode, ft

$\vec{R}$ position vector locating representative point on structural center line relative to inertial (H,R) frame, ft (see fig. 1)

$\vec{R}_o$ position vector locating center of gravity of launch vehicle relative to origin of inertial (H,R) frame, ft (see fig. 1)

$S(x)$ launch-vehicle cross-sectional area of revolution, sq ft

S_{cg} mass static unbalance of launch vehicle (less engines) about center of gravity, lb-sec^2

S_e, $S_{e,l}$ mass static unbalance of all engines and gimbaled engine, respectively, about gimbal point, lb-sec^2

S_o aerodynamic reference area, sq ft

s Laplace transform variable, sec^{-1}

T_e, $T_{e,l}$ total thrust of all engines and gimbaled engine, respectively, lb

T_v, $T_{v,l}$ total vacuum thrust of all engines and gimbaled engine, respectively, lb

T_l gimbaled engine load torques, ft-lb

t time, sec

U potential energy, ft-lb

$U(x_k-x_{b,n})$ unit step function

$u(x,t)$ elastic displacement of structural center line, $\sum_i \phi_i(x)\, q_i(t)$, ft

$\vec{V}_k$ velocity vector of particular slosh mass, ft/sec

V_m center-of-gravity velocity of launch vehicle, ft/sec

$V_{m,w}$	velocity of launch vehicle relative to wind, ft/sec
$\vec{V}_p$	velocity vector of point on deformed structural center line of launch vehicle, ft/sec
$\vec{V}_{p,1}$, $\vec{V}_{p,2}$	velocity vector of point on gimbaled and nongimbaled engines, respectively, ft/sec
V_s	velocity of sound at altitude h, ft/sec
V_x, V_y	component of center-of-gravity velocity vector along X- and Y-axis, respectively, ft/sec
V_w	wind velocity, ft/sec
V_1, V_2	relative velocity of exhaust particles to thrust chamber exit face, gimbaled and nongimbaled engines, respectively, ft/sec
$w(x,t)$	downwash, ft/sec
w_1, w_2	mass-flow rate through gimbaled and nongimbaled engines, respectively, lb-sec/ft
X,Y	body-fixed coordinate axes (see fig. 1)
x,y	coordinates along X and Y body axes, ft
$x_{b,n}$	coordinate of bending-moment station, ft
x_{cg}	center-of-gravity location, ft
x_k	propellant slosh mass location, ft
$x_\alpha, x_\theta, x_{\dot{\theta}}$	coordinate locating angle-of-attack sensor, attitude sensor, and attitude-rate sensor, respectively, ft
α	rigid-body angle of attack, $\theta - \gamma$, radians
α_s	angle of attack measured by angle-of-attack sensor, radians
α_w	wind-induced angle of attack, radians
β_i	arbitrary generalized coordinate
γ	flight-path angle - that is, angle velocity vector $\vec{V}_m$ makes with horizontal, radians
δ	gimbaled engine deflection angle (gimbal angle), radians

δ_c gimbaled engine command function, radians

ζ_i viscous damping ratio of ith bending mode

η_1, η_2 coordinate measured aft from gimbal point along gimbaled and non-gimbaled engines, respectively, ft

θ, θ_c attitude and attitude command angle, respectively, radians

θ_e error angle, $\theta_c - \theta_f$, radians

θ_f feedback angle, radians

λ_k propellant slosh coordinate as measured from deformed structural center line, ft

μ_1, μ_2 control system gains, sec and dimensionless, respectively

$\xi_{e,1}$ viscous damping ratio associated with gimbaled engine

ξ_f filter constant

ξ_k viscous damping ratio associated with propellant slosh modes

ρ atmospheric density at altitude h, $\frac{\text{lb-sec}^2}{\text{ft}^4}$

$\phi_i(x)$ displacement of ith mode

Ω_k slosh frequency parameter, $\text{radians}^2/\text{ft}$

ω_e gimbaled-engine constant, radians/sec

$\omega_{e,1}$ natural frequency of gimbaled engine, radians/sec

ω_f filter constant, radians/sec

ω_i natural frequency of ith bending mode, radians/sec

ω_k natural frequency of propellant slosh spring-mass systems, radians/sec

A dot over a variable indicates differentiation with respect to time.

A prime with a variable indicates differentiation with respect to x.

An arrow over a variable indicates a vector.

A bar over a variable indicates a Laplace transformation.

ANALYSIS

In this section the dynamical equations governing the planar motion of an ascending flexible launch vehicle are developed. The vehicle is considered to be autopilot controlled and subjected to the disturbing influence of atmospheric winds.

Mathematical Model

General.- The coordinate system used herein is illustrated in figure 1. Motion is referenced to a Cartesian coordinate system (x,y) fixed in the undeformed rigid body and oriented with respect to the flat earth horizontal by the attitude angle θ. Motion is constrained to the pitch plane. The center-of-gravity velocity vector $\vec{V}_m$ is oriented to the local horizontal by γ, the flight-path angle. The elastic displacement of the vehicle structure, relative to the undeformed center line (X-axis), is given by the function $u(x,t)$ which is discussed in the following section. Propellant sloshing is simulated by spring mass systems. Control forces are produced by swiveling the thrust chambers of all or some of the rocket engines through an angle δ in response to commands provided by an autopilot. The autopilot stabilizes the vehicle and guides it along a preprogramed flight path. External disturbances are assumed to come from horizontal winds whose relation to the center-of-gravity velocity vector is shown in the vector diagram of figure 1.

Bending modes.- Bending of a launch-vehicle structure is approximated by the center-line deflection of an equivalent free-free beam with nonuniform mass and stiffness properties. It is assumed that adequate representation is possible with the superposition of a finite number of terms in the series

$$u(x,t) = \sum_i \phi_i(x)\, q_i(t) \tag{1}$$

where $\phi_i(x)$ represents the free-free beam modes or eigenfunctions and $q_i(t)$ represents the related generalized coordinates. The mode shapes $\phi_i(x)$ are functions solely of the mass and stiffness properties exhibited at a particular time in the trajectory and represent known input quantities. The generalized coordinates $q_i(t)$ determine the contribution of each mode and, thus, represent independent degrees of freedom.

Several methods (for example, refs. 8 and 9) are available for the computation of the free-free bending modes. The derivation presented herein assumes

that the bending modes are computed at several discrete times in the ascent trajectory by using simple beam theory. The modes are thus orthogonal with respect to the weighting function $m(x,t)$, that is, running mass. Transverse shear and/or rotary inertia effects may be handled by including these second-order terms in the eigenvalue problem and modifying the generalized mass and orthogonality expressions accordingly (ref. 10). Bending modes are computed with engine masses uncoupled (removed) from the launch-vehicle structure and liquid propellants, if any, assumed frozen. Dynamical effects of the engine masses are included through inertial coupling in the equations of motion.

Propellant slosh.- A spring-mass analogy is employed to simulate liquid propellant motion. This analogy has been developed in the literature (refs. 1, 11, and 12, for example) for a variety of tank configurations. Essentially, the sloshing liquid is replaced by a spring-mounted mass which duplicates the resultant force exerted on the tank by the liquid when the fundamental slosh mode is excited at its resonant frequency. The parameters required by this representation are: slosh mass m_k, natural frequency ω_k, and slosh mass location x_k. These quantities are functions of the acceleration field and the ratio of fluid depth to tank radius and may be evaluated from information available in the previously cited literature. Viscosity, surface tension, and mechanical devices, such as baffles, provide sources of energy dissipation in sloshing liquids. For the analysis herein, an equivalent viscous damping factor ξ_k has been inserted in each slosh degree of freedom. Approximate values of this parameter may be established on the basis of information available in the previously mentioned sources or from experimental investigations (for example, refs. 13 and 14).

Method of Analysis

The derivation of the equations of motion is based on the results of a variational procedure (ref. 7) developed from momentum considerations. Part of the variational principle, as stated therein, is readily recognized as having the same form as Lagrange's equations and it will be these operations that are presented in this section. However, whereas the classical derivation of Lagrange's equations is based on the assumption of constant mass, no such requirement is imposed on the operations implied by the variational principle presented in reference 7. Hereafter, the term "Lagrange's equations" will be interpreted as having the same meaning as established in the context of reference 7. In addition, it should be noted that the variational principle cited yields equivalent generalized force terms (appendix C) which account for the distributed loading exerted on a launch-vehicle structure by the internal momentum flux of the flowing propellants. The distributed loading, when integrated, yields the principle thrust terms and additional contributions which account for the dynamic coupling of the propellant flow. Although treated in appendix C, these effects are excluded from the equations of motion.

Lagrange's equations.- A general form of Lagrange's equations suitable for variable mass systems and expressed in the classical form, that is, referenced to an inertial (space-fixed) frame has been developed in reference 7. For the

analysis presented herein, it is convenient to reference the motion of the launch vehicle to the rotating frame (X,Y) illustrated in figure 1. The classical expression of Lagrange's equations must therefore be transformed to a form which is valid in the rotating coordinate system. Details of the transformation may be obtained from references 15 and 16. (A similar, but less general, form is summarized in ref. 17.) When transformed, Lagrange's equations for the rigid-body degrees of freedom (translation and pitch) assume the following forms:

$$\frac{d}{dt}\frac{\partial E}{\partial V_x} - \dot{\theta}\frac{\partial E}{\partial V_y} + \sin\theta\,\frac{\partial U}{\partial h} = \sum F_x \tag{2a}$$

$$\frac{d}{dt}\frac{\partial E}{\partial V_y} + \dot{\theta}\frac{\partial E}{\partial V_x} + \cos\theta\,\frac{\partial U}{\partial h} = \sum F_y \tag{2b}$$

$$\frac{d}{dt}\frac{\partial E}{\partial \dot{\theta}} + V_x\frac{\partial E}{\partial V_y} - V_y\frac{\partial E}{\partial V_x} + \frac{\partial U}{\partial \theta} = \sum M_{cg} \tag{2c}$$

where U has been assumed independent of r.

Lagrange's equations for the remaining degrees of freedom (bending, propellant slosh, and gimbaled engine) remain unchanged when transformed and have the form

$$\frac{d}{dt}\frac{\partial E}{\partial \dot{\beta}_i} - \frac{\partial E}{\partial \beta_i} + \frac{\partial U}{\partial \beta_i} + \frac{\partial D}{\partial \dot{\beta}_i} = \sum_i Q_{\beta i} \tag{3}$$

where β_i represents a particular coordinate (degree of freedom), and a dissipation function D has been added.

Kinetic energy.- The derivation is initiated by writing the total kinetic energy of the system. It is assumed that the mass of the vehicle is distributed along the structural center line. From coordinate system considerations (as illustrated in fig. 1), the position vector locating a point on the structural center line relative to the origin of the inertial frame (H,R) is given by

$$\vec{R} = \vec{R}_o + \vec{i}(x - x_{cg}) + \vec{j}\sum_i \phi_i(x)\, q_i(t)$$

where $\phi_i(x)$ represents the orthogonal free-free mode shapes and $q_i(t)$ represents the associated generalized coordinates. The vector $\vec{R}_o$, expressed in space-fixed components, locates the center of gravity of the launch vehicle relative to the inertial origin. Perturbations of the center of gravity normal

to the vehicle center line resulting from displacements of the structure, engines, and propellant slosh masses are neglected.

The absolute velocity vector $\vec{V}_p$ of a point on the structural center line may be determined by differentiating the position vector $\vec{R}$. Since the body axes (X,Y) rotate, this differentiating must account for the time rate of change of the direction of the unit vectors $\vec{i}$ and $\vec{j}$. Differentiating $\vec{R}$ and noting that

$$\frac{d\vec{i}}{dt} = \vec{j}\dot{\theta}$$

$$\frac{d\vec{j}}{dt} = -\vec{i}\dot{\theta}$$

produces the following equation for the velocity vector $\vec{V}_p$:

$$\vec{V}_p = \frac{d\vec{R}}{dt} = \dot{\vec{R}}_o + \vec{i}\left[-\dot{x}_{cg} - \dot{\theta} \sum_i \phi_i(x)\, q_i(t)\right] + \vec{j}\left[\dot{\theta}(x - x_{cg}) + \sum_i \phi_i(x)\, \dot{q}_i(t)\right]$$

If the absolute velocity vector $\dot{\vec{R}}_o$ of the center of gravity is instantaneously resolved into components along the body-fixed (X,Y) axes, that is,

$$\dot{\vec{R}}_o = \vec{i}V_x + \vec{j}V_y$$

the vector $\vec{V}_p$ may be expressed in the following form:

$$\vec{V}_p = \vec{i}\left[V_x - \dot{x}_{cg} - \dot{\theta} \sum_i \phi_i(x)\, q_i(t)\right] + \vec{j}\left[V_y + \dot{\theta}(x - x_{cg}) + \sum_i \phi_i(x)\, \dot{q}_i(t)\right] \tag{4}$$

With the assumption of small engine rotation angles and elastic deformations, the absolute velocity vector $\vec{V}_{p,l}$ of a representative point on the gimbaled engine may be determined in a similar manner and is given by the following equation:

$$\vec{V}_{p,1} = \vec{i}\left\{V_x - \dot{x}_{cg} - \dot{\theta}\eta_1\left[\delta - \sum_i \phi_i'(0)\, q_i(t)\right] - \dot{\theta}\sum_i \phi_i(0)\, q_i(t) + \eta_1\left[\delta - \sum_i \phi_i'(0)\, q_i(t)\right]\left[\dot{\delta} - \sum_i \phi_i'(0)\, \dot{q}_i(t)\right]\right\}$$

$$+ \vec{j}\left\{V_y - \dot{\theta}\left(x_{cg} + \eta_1\right) + \sum_i \phi_i(0)\, \dot{q}_i(t) + \eta_1\left[\dot{\delta} - \sum_i \phi_i'(0)\, \dot{q}_i(t)\right]\right\} \tag{5}$$

The velocity vector $\vec{V}_{p,2}$ for a point on the center line of the nongimbaled engine may be obtained from equation (5) simply by nulling the gimbaled engine deflection angle ($\delta = 0$) and is given as follows:

$$\vec{V}_{p,2} = \vec{i}\left[V_x - \dot{x}_{cg} + \eta_2\dot{\theta}\sum_i \phi_i'(0)\, q_i(t) - \dot{\theta}\sum_i \phi_i(0)\, q_i(t) + \eta_2\sum_i\sum_j \phi_i'(0)\,\phi_j'(0)\, q_i(t)\, \dot{q}_j(t)\right]$$

$$+ \vec{j}\left[V_y - \dot{\theta}\left(x_{cg} + \eta_2\right) + \sum_i \phi_i(0)\, \dot{q}_i(t) - \eta_2\sum_i \phi_i'(0)\, \dot{q}_i(t)\right] \tag{6}$$

In addition, the absolute velocity vector $\vec{V}_k$ of a representative slosh mass is required and is given as follows:

$$\vec{V}_k = \vec{V}_p - \dot{\theta}\lambda_k\vec{i} + \dot{\lambda}_k\vec{j} \tag{7}$$

With the use of equations (4) to (7), the total kinetic energy of the configuration may be formulated as

$$E = \frac{1}{2}\int_0^L \left(\vec{V}_p \cdot \vec{V}_p\right) m(x,t)\, dx + \frac{1}{2}\int_0^{d_2}\left(\vec{V}_{p,2} \cdot \vec{V}_{p,2}\right) m(\eta_2)\, d\eta_2 + \frac{1}{2}\int_0^{d_1}\left(\vec{V}_{p,1} \cdot \vec{V}_{p,1}\right) m(\eta_1)\, d\eta_1$$

$$+ \frac{1}{2}\sum_k m_k\left\{\dot{\theta}^2\lambda_k^2 - 2\dot{\theta}\lambda_k\left[V_x - \dot{\theta}\sum_i \phi_i(x_k) q_i(t) - \dot{x}_{cg}\right] + \dot{\lambda}_k^2 + 2\dot{\lambda}_k\left[V_y + \dot{\theta}\left(x_k - x_{cg}\right) + \sum_i \phi_i(x_k)\, \dot{q}_i(t)\right]\right\} \tag{8}$$

It is convenient to define certain integral forms and combinations thereof which occur frequently in the ensuing development. The following definitions are established:

$$m_{e,1} = \int_0^{d_1} m(\eta_1)\, d\eta_1 \tag{9a}$$

$$m_e = \int_0^{d_2} m(\eta_2)\, d\eta_2 + m_{e,1} \tag{9b}$$

$$m_t = \int_0^{L} m(x,t)\, dx + m_e \tag{9c}$$

$$\left.\begin{aligned} m_i &= \int_0^{L} m(x,t)\, \phi_i(x)\, \phi_j(x)\, dx \qquad (i = j) \\ m_i &= 0 \qquad\qquad\qquad\qquad\qquad\quad (i \neq j) \end{aligned}\right\} \tag{9d}$$

$$S_{e,1} = \int_0^{d_1} \eta_1 m(\eta_1)\, d\eta_1 \tag{9e}$$

$$S_e = \int_0^{d_2} \eta_2 m(\eta_2)\, d\eta_2 + S_{e,1} \tag{9f}$$

$$S_{cg} = \int_0^{L} (x - x_{cg}) m(x,t)\, dx \tag{9g}$$

$$I_{e,1} = \int_0^{d_1} \eta_1^2 m(\eta_1)\, d\eta_1 \tag{9h}$$

$$I_e = \int_0^{d_2} \eta_2^2 m(\eta_2)\, d\eta_2 + I_{e,1} \tag{9i}$$

$$I_{cg} = \int_0^{L} m(x,t)(x - x_{cg})^2\, dx \tag{9j}$$

$$S_{cg} - (m_e x_{cg} + S_e) = 0 \tag{9k}$$

$$\int_0^{L} m(x,t)\, \phi_i(x)\, dx = 0 \tag{9l}$$

$$\int_0^{L} (x - x_{cg}) m(x,t)\, \phi_i(x)\, dx = 0 \tag{9m}$$

Potential energy and dissipation function.- If engine rotation angles and elastic deformations are assumed small, as was done previously, the potential energy of the system may be written as follows:

$$U = \frac{1}{2}\sum_i m_i\omega_i^2 q_i^2(t) + \frac{1}{2}\sum_k m_k\omega_k^2\lambda_k^2 + \frac{1}{2} I_{e,1}\omega_{e,1}^2\delta^2 + g\int_0^L \left[h + (x - x_{cg})\sin\theta + \cos\theta \sum_i \phi_i(x)\, q_i(t)\right] m(x,t)\, dx + g\cos\theta \sum_k m_k\lambda_k$$

$$+ g\int_0^{d_1}\left\{h - x_{cg}\sin\theta + \cos\theta\sum_i \phi_i(o)\, q_i(t) + \eta_1\cos\theta\left[\delta - \sum_i \phi_i'(o)\, q_i(t)\right] - \eta_1\sin\theta\right\} m(\eta_1)\, d\eta_1 + g\int_0^{d_2}\left[h - x_{cg}\sin\theta\right.$$

$$\left. + \cos\theta\sum_i \phi_i(o)\, q_i(t) - \eta_2\cos\theta\sum_i \phi_i'(o)\, q_i(t) - \eta_2\sin\theta\right] m(\eta_2)\, d\eta_2 \qquad (10)$$

The first three terms in equation (10) represent, respectively, the deformational strain energy (refs. 5, 8, and 10) of the structure, the strain energy of the propellant slosh spring mass systems, and the strain energy of the gimbaled engine backup structure and positioning actuator. Remaining terms in the expression for U define the gravitational potential. With the use of equations (9), the potential U may be reduced to the following form:

$$U = m_t g h + \frac{1}{2}\sum_i m_i\omega_i^2 q_i^2(t) + \sum_k m_k\left(\frac{1}{2}\omega_k^2\lambda_k^2 + g\lambda_k\cos\theta\right) + \frac{1}{2} I_{e,1}\omega_{e,1}^2\delta^2 + g\cos\theta\left[m_e\sum_i \phi_i(o)\, q_i(t) + S_{e,1}\delta - S_e\sum_i \phi_i'(o)\, q_i(t)\right] \qquad (11)$$

It is convenient to account for the dissipative (damping) forces through a velocity dependent potential. (See ref. 18.) The dissipation function D for the system is assumed in the following form:

$$D = \sum_i m_i\zeta_i\omega_i\dot{q}_i^2(t) + \sum_k m_k\omega_k\xi_k\dot{\lambda}_k^2 + I_{e,1}\xi_{e,1}\omega_{e,1}\dot{\delta}^2 \qquad (12)$$

Structural damping, as represented by the first term in equation (12), is treated as an equivalent viscous type (refs. 1 and 5) and is justified on the basis that the structural modes are lightly damped with little dissipative cross-coupling. The second term in equation (12) gives the propellant slosh damping forces, as discussed previously. Dissipative effects associated with the gimbaled engine backup structure and positioning actuator are, likewise, treated as an equivalent viscous type.

Equations of Motion

The equations of motion are derived by means of a modified form of Lagrange's equations (eqs. (2) and (3)). Application of the equations is illustrated by a detailed derivation of the equation governing motion along the X body axis. Equations for the remaining degrees of freedom may be obtained in a similar manner and are merely stated after dropping negligible terms. The control system equations and expressions for the applied forces are developed in subsequent sections. The equations are summarized in appendix E.

Axial motion equation.- The differential equation governing motion of the launch vehicle along the X body axis may be obtained from the application of equation (2a). The first term in equation (2a) requires determining the partial derivative of the kinetic energy E with respect to the velocity V_x; that is,

$$\frac{\partial E}{\partial V_x} = \int_0^L \left(\vec{V}_p \cdot \frac{\partial \vec{V}_p}{\partial V_x}\right) m(x,t)\, dx + \int_0^{d_2} \left(\vec{V}_{p,2} \cdot \frac{\partial \vec{V}_{p,2}}{\partial V_x}\right) m(\eta_2)\, d\eta_2 + \int_0^{d_1} \left(\vec{V}_{p,1} \cdot \frac{\partial \vec{V}_{p,1}}{\partial V_x}\right) m(\eta_1)\, d\eta_1 - \dot{\theta} \sum_k m_k \lambda_k \tag{13}$$

From equations (4), (5), and (6) the partial derivatives

$$\left.\begin{aligned} \frac{\partial \vec{V}_p}{\partial V_x} &= \vec{i} \\ \frac{\partial \vec{V}_{p,1}}{\partial V_x} &= \vec{i} \\ \frac{\partial \vec{V}_{p,2}}{\partial V_x} &= \vec{i} \end{aligned}\right\} \tag{14}$$

may be obtained and when substituted into equation (13) produce the following equation:

$$\begin{aligned} \frac{\partial E}{\partial V_x} = \int_0^L \left[V_x - \dot{x}_{cg} - \dot{\theta} \sum_i \phi_i(x)\, q_i(t)\right] m(x,t)\, dx + \int_0^{d_2} \Bigg[V_x - \dot{x}_{cg} + \eta_2 \dot{\theta} \sum_i \phi_i'(0)\, q_i(t) - \dot{\theta} \sum_i \phi_i(0)\, q_i(t) \\ + \eta_2 \sum_i \sum_j \phi_i'(0)\, \phi_j'(0)\, q_i(t)\, \dot{q}_j(t)\Bigg] m(\eta_2)\, d\eta_2 + \int_0^{d_1} \Bigg\{V_x - \dot{x}_{cg} - \eta_1 \dot{\theta}\left[\delta - \sum_i \phi_i'(0)\, q_i(t)\right] - \dot{\theta} \sum_i \phi_i(0)\, q_i(t) \\ + \eta_1 \left[\delta - \sum_i \phi_i'(0)\, q_i(t)\right]\left[\dot{\delta} - \sum_i \phi_i'(0)\, \dot{q}_i(t)\right]\Bigg\} m(\eta_1)\, d\eta_1 - \dot{\theta} \sum_k m_k \lambda_k \end{aligned}$$

When the previously established definitions given by equations (9) are used, the integrations can be performed and the expression for $\partial E/\partial V_x$ reduced to the following form:

$$\frac{\partial E}{\partial V_x} = m_t\left(V_x - \dot{x}_{cg}\right) - m_e\dot{\theta}\sum_i \phi_i(0)\, q_i(t) - S_{e,1}\dot{\theta}\delta + S_e\dot{\theta}\sum_i \phi_i'(0)\, q_i(t)$$

$$+ S_{e,1}\delta\dot{\delta} - S_{e,1}\delta\sum_i \phi_i'(0)\,\dot{q}_i(t) - S_{e,1}\dot{\delta}\sum_i \phi_i'(0)\, q_i(t)$$

$$+ S_e\sum_i\sum_j \phi_i'(0)\,\phi_j'(0)\, q_i(t)\,\dot{q}_j(t) - \dot{\theta}\sum_k m_k\lambda_k \qquad (15)$$

Lagrange's equation (eq. (2a)) also requires the first time derivative of equation (15). In carrying out this operation, it should be noted that the analytical foundation for the propellant slosh analogy requires that the parameters m_k, ω_k, x_k, and ξ_k be treated as quasi-steady functions. Differentiating equation (15) with respect to time produces the following equation:

$$\frac{d}{dt}\frac{\partial E}{\partial V_x} = m_t\left(\dot{V}_x - \ddot{x}_{cg}\right) + \dot{m}_t\left(V_x - \dot{x}_{cg}\right) - m_e\left[\dot{\theta}\sum_i \phi_i(0)\,\dot{q}_i(t) + \ddot{\theta}\sum_i \phi_i(0)\, q_i(t)\right] + S_e\left[\ddot{\theta}\sum_i \phi_i'(0)\, q_i(t) + \dot{\theta}\sum_i \phi_i'(0)\,\dot{q}_i(t)\right]$$

$$+ S_e\left\{\left[\sum_i \phi_i'(0)\,\dot{q}_i(t)\right]^2 + \sum_i\sum_j \phi_i'(0)\,\phi_j'(0)\, q_i(t)\,\ddot{q}_j(t)\right\} + S_{e,1}\left(\delta\ddot{\delta} + \dot{\delta}^2\right) - S_{e,1}\left(\dot{\theta}\dot{\delta} + \ddot{\theta}\delta\right) - S_{e,1}\left[2\dot{\delta}\sum_i \phi_i'(0)\,\dot{q}_i(t)\right.$$

$$\left. + \delta\sum_i \phi_i'(0)\,\ddot{q}_i(t)\right] - S_{e,1}\left[\ddot{\delta}\sum_i \phi_i'(0)\, q_i(t)\right] - \sum_k m_k\left(\dot{\theta}\dot{\lambda}_k + \ddot{\theta}\lambda_k\right) \qquad (16)$$

In a similar manner the partial derivative of the kinetic energy with respect to the velocity V_y may be obtained as follows:

$$\frac{\partial E}{\partial V_y} = m_t V_y + m_e\sum_i \phi_i(0)\,\dot{q}_i(t) + S_{e,1}\dot{\delta} - S_e\sum_i \phi_i'(0)\,\dot{q}_i(t) + \sum_k m_k\dot{\lambda}_k \qquad (17)$$

Finally, the partial derivative of the potential U (eq. (11)) with respect to the altitude h produces the gravity force as follows:

$$\frac{\partial U}{\partial h} = m_t g \qquad (18)$$

In order to simplify the equations, all triple product combinations of $\dot{\theta}$, $\ddot{\theta}$, and zero, first, and second order time derivatives of δ, $\sum_i \phi_i(0)\, q_i(t)$, and $\sum_i \phi_i'(0)\, q_i(t)$ are eliminated from the final equations. Substituting

equations (16), (17), and (18) into equation (2a) produces the following equation governing motion along the X body axis:

$$m_t\left(\dot{V}_x - \ddot{x}_{cg}\right) + \dot{m}_t\left(V_x - \dot{x}_{cg}\right) - m_e\left[2\dot{\theta}\sum_i \phi_i(0)\,\dot{q}_i(t) + \ddot{\theta}\sum_i \phi_i(0)\,q_i(t)\right] - S_{e,1}\left(2\dot{\theta}\dot{\delta} + \ddot{\theta}\delta\right) + S_e\left[2\dot{\theta}\sum_i \phi_i'(0)\,\dot{q}_i(t) + \ddot{\theta}\sum_i \phi_i'(0)\,q_i(t)\right]$$

$$+ S_{e,1}\left(\delta\ddot{\delta} + \dot{\delta}^2\right) - S_{e,1}\left[2\dot{\delta}\sum_i \phi_i'(0)\,\dot{q}_i(t) + \delta\sum_i \phi_i'(0)\,\ddot{q}_i(t) + \ddot{\delta}\sum_i \phi_i'(0)\,q_i(t)\right] + S_e\left\{\sum_i\sum_j \phi_i'(0)\,\phi_j'(0)\left[\dot{q}_i(t)\,\dot{q}_j(t) + q_i(t)\,\ddot{q}_j(t)\right]\right\}$$

$$- \sum_k m_k\left(2\dot{\theta}\dot{\lambda}_k + \ddot{\theta}\lambda_k\right) - m_t\dot{\theta}V_y + m_t g\sin\theta = \sum F_x \qquad (19)$$

where the right-hand side, that is, $\sum F_x$, represents the summation of the x-components of all the applied forces not accounted for in the potential U. It should be noted that the constituents of the term $\sum F_x$ account for the aerodynamic and propulsive forces and are discussed in a subsequent section.

Lateral motion equation.- With the use of equation (2b), the equation governing motion along the Y body axis is obtained as

$$m_t\dot{V}_y + \dot{m}_t V_y + m_e\sum_i \phi_i(0)\,\ddot{q}_i(t) + S_{e,1}\ddot{\delta} - S_e\sum_i \phi_i'(0)\,\ddot{q}_i(t) + \sum_k m_k\ddot{\lambda}_k - \dot{\theta}^2\sum_k m_k\lambda_k + m_t\left(V_x - \dot{x}_{cg}\right)\dot{\theta} + m_t g\cos\theta = \sum F_y \qquad (20)$$

where the term $\sum F_y$ represents the summation of the y-components of all the applied forces not accounted for in the potential U.

Pitch equation.- Finally, the remaining rigid-body equation representing pitching motion of the launch vehicle about its center of gravity is obtained by using equation (2c) and is

$$I_{cg}\ddot{\theta} + \dot{I}_{cg}\dot{\theta} + m_e x_{cg}^2\ddot{\theta} + 2S_e x_{cg}\ddot{\theta} + I_e\ddot{\theta} - m_e\left(\dot{V}_x - \ddot{x}_{cg}\right)\sum_i \phi_i(0)\,q_i(t) - S_{e,1}\left(\dot{V}_x - \ddot{x}_{cg}\right)\delta + S_e\left(\dot{V}_x - \ddot{x}_{cg}\right)\sum_i \phi_i'(0)\,q_i(t)$$

$$- m_e x_{cg}\sum_i \phi_i(0)\,\ddot{q}_i(t) - S_e\sum_i \phi_i(0)\,\ddot{q}_i(t) - S_{e,1}x_{cg}\ddot{\delta} + S_e x_{cg}\sum_i \phi_i'(0)\,\ddot{q}_i(t) - I_{e,1}\ddot{\delta} + I_e\sum_i \phi_i'(0)\,\ddot{q}_i(t)$$

$$+ \sum_k m_k\left[\ddot{\lambda}\left(x_k - x_{cg}\right) - \left(\dot{V}_x - \ddot{x}_{cg}\right)\lambda_k\right] + m_e V_y\dot{\theta}\sum_i \phi_i(0)\,q_i(t) + S_{e,1}V_y\dot{\theta}\delta - S_e V_y\dot{\theta}\sum_i \phi_i'(0)\,q_i(t) - S_{e,1}\delta\dot{V}_y$$

(Equation continued on next page)

$$+ S_{e,1}\delta V_y \sum_i \phi_i'(0)\,\dot{q}_i(t) + S_{e,1}V_y\dot{\delta} \sum_i \phi_i'(0)\,q_i(t) - S_eV_y \sum_i \sum_j \phi_i'(0)\,\phi_j'(0)\,q_i(t)\,\dot{q}_j(t) + V_y\dot{\theta} \sum_k m_k\lambda_k$$

$$+ \ddot{\theta} \sum_i m_i q_i^2(t) + 2\dot{\theta} \sum_i m_i q_i(t)\,\dot{q}_i(t) + \dot{\theta} \sum_i \dot{m}_i q_i^2(t) + \ddot{\theta} \sum_k m_k\lambda_k^2 + 2\dot{\theta} \sum_k m_k\lambda_k\dot{\lambda}_k + 2\ddot{\theta} \sum_k \sum_i m_k\lambda_k\phi_i(x_k)\,q_i(t)$$

$$+ 2\dot{\theta} \sum_k \sum_i m_k\dot{\lambda}_k\phi_i(x_k)\,q_i(t) + 2\dot{\theta} \sum_k \sum_i m_k\lambda_k\phi_i(x_k)\,\dot{q}_i(t) + m_tV_y\dot{x}_{cg} + 2\dot{x}_{cg}\dot{\theta}\left(m_ex_{cg} + S_e\right) - g\sin\theta \sum_k m_k\lambda_k$$

$$- g\sin\theta\left[m_e \sum_i \phi_i(0)\,q_i(t) + S_{e,1}\delta - S_e \sum_i \phi_i'(0)\,q_i(t)\right] = \sum M_{cg} \tag{21}$$

The quantity $\sum M_{cg}$ represents the summation of the moments of the applied forces about the center of gravity.

Bending mode equation.- The equation of motion for the jth bending mode is determined by replacing β_i in equation (3) by the coordinate q_j, that is,

$$\frac{d}{dt}\frac{\partial E}{\partial \dot{q}_j} - \frac{\partial E}{\partial q_j} + \frac{\partial U}{\partial q_j} + \frac{\partial D}{\partial \dot{q}_j} = \sum_j Q_{qj} \tag{22}$$

where j assumes the successive values 1, 2, 3, . . . up to the number of terms employed in the series $\sum_i \phi_i(x)\,q_i(t)$ (eq. (1)). Using the results of equations (9) and neglecting the higher order terms, as was done previously, gives the jth bending mode equation in the following form:

$$m_j\ddot{q}_j(t) + 2m_j\zeta_j\omega_j\dot{q}_j(t) + m_j\omega_j^2q_j(t) + \dot{m}_j\dot{q}_j(t) - \left(\dot{V}_x - \ddot{x}_{cg}\right)S_{e,1}\delta\phi_j'(0) + \left(\dot{V}_x - \ddot{x}_{cg}\right)S_e\phi_j'(0) \sum_i \phi_i'(0)\,q_i(t) + m_e\phi_j(0)\dot{V}_y - m_ex_{cg}\phi_j(0)\ddot{\theta}$$

$$- S_e\phi_j(0)\ddot{\theta} + m_e\phi_j(0) \sum_i \phi_i(0)\,\ddot{q}_i(t) + S_{e,1}\phi_j(0)\ddot{\delta} - S_e\phi_j(0) \sum_i \phi_i'(0)\,\ddot{q}_i(t) - S_e\phi_j'(0)\dot{V}_y + S_ex_{cg}\phi_j'(0)\ddot{\theta} + I_e\phi_j'(0)\ddot{\theta}$$

$$- S_e\phi_j'(0) \sum_i \phi_i(0)\,\ddot{q}_i(t) - I_{e,1}\phi_j'(0)\ddot{\delta} + I_e\phi_j'(0) \sum_i \phi_i'(0)\,\ddot{q}_i(t) + \sum_k m_k\phi_j(x_k)\ddot{\lambda}_k - S_e\left(V_x - 2\dot{x}_{cg}\right)\dot{\theta}\phi_j'(0) + m_e\left(V_x - 2\dot{x}_{cg}\right)\dot{\theta}\phi_j(0)$$

$$- m_jq_j(t)\dot{\theta}^2 + m_eg\phi_j(0)\cos\theta - S_eg\phi_j'(0)\cos\theta - \dot{\theta}^2 \sum_k m_k\lambda_k\phi_j(x_k) = \sum_j Q_{qj} \tag{23}$$

The generalized force $\sum Q_{q_j}$ associated with the jth bending mode will be developed in a subsequent section.

Propellant slosh equation.- The propellant slosh equation is determined similarly from equation (3) by replacing β_i with the coordinate λ_k. Since the slosh masses are excited solely by dynamic coupling and not by any external sources, the results are equated to zero. When the indicated operations are performed, the equation of motion for the propellant slosh coordinate λ_k reduces to

$$m_k\ddot{\lambda}_k + 2m_k\xi_k\omega_k\dot{\lambda}_k + m_k\omega_k^2\lambda_k + m_k\dot{V}_y + m_k\ddot{\theta}(x_k - x_{cg}) + m_k\sum_i \phi_i(x_k)\,\ddot{q}_i(t) - m_k\dot{\theta}^2\sum_i \phi_i(x_k)\,q_i(t) - m_k\lambda_k\dot{\theta}^2$$

$$+ m_k\dot{\theta}(V_x - 2\dot{x}_{cg}) + m_k g\cos\theta = 0 \qquad (24)$$

where k assumes the successive values 1, 2, 3, . . . up to the number of independent slosh degrees of freedom utilized.

Gimbaled engine equation.- The equation of motion for the gimbaled engine is obtained by replacing β_i in equation (3) with the coordinate δ:

$$I_{e,1}\ddot{\delta} + 2I_{e,1}\xi_{e,1}\omega_{e,1}\dot{\delta} + I_{e,1}\omega_{e,1}^2\delta = Q_\delta + T_l \qquad (25)$$

where the load torques T_l are given by the following equation:

$$T_l = I_{e,1}\sum_i \phi_i'(0)\,\ddot{q}_i(t) - S_{e,1}(\dot{V}_x - \ddot{x}_{cg})\delta + S_{e,1}(\dot{V}_x - \ddot{x}_{cg})\sum_i \phi_i'(0)\,q_i(t) - S_{e,1}\dot{V}_y + S_{e,1}\ddot{\theta}x_{cg} + I_{e,1}\ddot{\delta} - S_{e,1}\sum_i \phi_i(0)\,\ddot{q}_i(t)$$

$$- S_{e,1}(V_x - 2\dot{x}_{cg})\dot{\theta} - S_{e,1}g\cos\theta \qquad (26)$$

The generalized force, or control torque, Q_δ is discussed in the section entitled "Gimbaled Engine Commands."

Control Equations

Feedback considerations.- The general mathematical description of a launch-vehicle control system is not attempted due to the wide variety presently employed. A typical control system is shown in figure 2. The input to the loop is a pitch command θ_c which serves as an attitude reference during flight. Three types of control sensors are indicated. These are: (1) an attitude sensor located at coordinate x_θ, (2) an attitude rate sensor located at coordinate $x_{\dot{\theta}}$, and (3) an angle-of-attack measuring device located at coordinate x_α. These instruments not only sense the rigid motion, but in addition, due to flexing of the vehicle's structure respond to local changes in

the slope and displacement of the structural center line. That part of the feedback signal θ_f proportional to local bending motion is commonly termed "the structural feedback" and is associated with many structural dynamic problems in launch vehicles.

Transforming from the frequency plane to the time domain, the feedback equation may be written as

$$\theta_f = \theta + \sum_i \phi_i'(x_\theta)\, q_i(t) + \mu_1 \left[\dot{\theta} + \sum_i \phi_i'(x_{\dot{\theta}})\, \dot{q}_i(t) \right] + \mu_2 \alpha_s \tag{27}$$

where the local measured angle of attack is given by the following equation:

$$\alpha_s = \alpha + \alpha_w + \sum_i \phi_i'(x_\alpha)\, q_i(t) - \frac{1}{V_{m,w}} \left[\dot{\theta}\left(x_\alpha - x_{cg}\right) + \sum_i \phi_i(x_\alpha)\, \dot{q}_i(t) \right] \tag{28}$$

In equations (27) and (28), the terms proportional to $q_i(t)$ and $\dot{q}_i(t)$ represent the structural feedback.

A filter-amplifier network is included in the forward loop of the control system for compensation. In parallel with the filter is an integrator to reduce steady-state errors. The filter equations may be written as follows:

$$\left.\begin{aligned} \ddot{\delta}_c + 2\xi_f \omega_f \dot{\delta}_c + \omega_f^2 \delta_c &= a_o \left[K_f \dot{\theta}_e + \omega_f \left(\omega_f + 2K_f \xi_f \right) \theta_e + K_f \omega_f^2 \int_0^t \theta_e \, dt \right] \\ \theta_e &= \theta_c - \theta_f \end{aligned}\right\} \tag{29}$$

Gimbaled engine commands.- The gimbaled thrust chamber or engine is positioned by an actuator in response to commands from the control system. Generally, the positioning actuator is some sort of electrohydraulic system which exhibits a nonlinear response for small amplitude oscillations. However, the type of nonlinearities involved - gimbal coulomb friction and fluid flow and compressibility effects, for example - are amenable to analysis by linearization processes such as the describing function method. Reference 20 is such an analysis and indicates that the generalized force, or applied corrective torque, Q_δ exerted on the engine by the actuator may be expressed in the following form:

$$Q_\delta = I_{e,1} K_c \omega_e^2 \int_0^t (\delta_c - \delta)\, dt + K_o \int_0^t T_l \, dt \tag{30}$$

where the commanded engine attitude is δ_c (fig. 3) and the engine load torques T_l are given by equation (26). It should be noted that equation (30) implicitly assumes that the actuator does not exert a moment on the structure. Combining the results of equation (30) with the previous results of equation (25) produces the following linear equation governing motion of the gimbaled engine.

$$\ddot{\delta} + 2\xi_{e,1}\omega_{e,1}\dot{\delta} + \omega_{e,1}^2\delta = K_c\omega_e^2 \int_0^t (\delta_c - \delta)\, dt + \frac{T_l}{I_{e,1}} + \frac{K_o}{I_{e,1}} \int_0^t T_l\, dt \quad (31)$$

Equation (31) characterizes the engine response as consisting of a second-order oscillatory component plus a lag and in this sense the parameters $\xi_{e,1}$ and $\omega_{e,1}$ have been interpreted as the viscous damping and natural frequency of the idealized system. In reality, however, these paramters, as well as K_c and K_o, are determined from a describing function analysis of the nonlinear actuator. Other forms of the control torque Q_δ may be used depending upon the degree of sophistication required and upon the characteristics of the particular system being investigated; examples may be found in the literature. (See, for example, refs. 1, 5, 10, and 12.)

In addition, a torque is exerted on the thrust chamber by virtue of its motion and the mass flow of the exhaust gases. An expression for this torque, which may be categorized as a jet damping effect, is developed in appendix C (eq. (C17)); however, its contribution in equation (31) is neglected.

Forces Acting on the Launch Vehicle

Propulsive forces.- Equations for the propulsive forces and moments associated with a launch vehicle employing a single gimbaled thrust chamber, are derived in appendix C. The propulsive forces evolve from a consideration of the internal momentum flux which yields a distributed loading proportional to the local propellant mass flow (eqs. (C1) to (C5)). The distributed loading, when integrated, yields the principle propulsive forces and moments and additional terms which account for the integrated effect of the internal propellant mass transfer.

The results presented in appendix C are easily amended to handle the situation of both gimbaled and nongimbaled engines. In the ensuing development, parameters associated with the gimbaled engine are denoted by the subscript 1, whereas parameters associated with the nongimbaled engine are denoted by the subscript 2. Parameters common to both engines appear without a numerical subscript. The following definitions are used:

$$\left.\begin{aligned} \dot{m}_t &= w_1 + w_2 \\ T_{e,1} &= T_{v,1} - A_1 p_o \\ T_e &= T_v - (A_1 + A_2) p_o \end{aligned}\right\} \quad (32)$$

where $T_{v,1}$ and T_v represent the rated vacuum thrust of the gimbaled engine and all engines, respectively, and are defined by the following two equations:

$$\left.\begin{aligned} T_{v,1} &= -w_1 V_1 + A_1 p_{e,1} \\ T_v &= T_{v,1} - w_2 V_2 + A_2 p_{e,2} \end{aligned}\right\} \tag{33}$$

It should be noted that $\dot{m}_t$, w_1, and w_2 are negative quantities.

Using the results of equations (32) and (33) and retaining only the principle thrust terms and the mass-flow-rate terms which cancel with similar terms in equation (19), the component of the propulsive force along the X body axis may be approximated on the basis of equation (C7).

$$F_{p,x} = T_e + \dot{m}_t\left(V_x - \dot{x}_{cg}\right) \tag{34}$$

In a similar manner the remaining propulsive forces and moments may be constructed and are listed as follows:

$$\left.\begin{aligned} F_{p,y} &= -T_{e,1}\delta + T_e \sum_i \phi_i'(0)\, q_i(t) + \dot{m}_t V_y \\ M_p &= T_{e,1} x_{cg}\delta - T_e x_{cg} \sum_i \phi_i'(0)\, q_i(t) - T_e \sum_i \phi_i(0)\, q_i(t) \\ Q_{j,p} &= -T_{e,1}\phi_j(0)\delta + T_e \phi_j(0) \sum_i \phi_i'(0)\, q_i(t) \end{aligned}\right\} \tag{35}$$

Aerodynamic forces.- Two methods for approximating the lift distribution on a slender deforming body are summarized herein. Slender-body momentum theory, as developed in appendix A, provides both a steady and unsteady contribution to the aerodynamic loading but does not include Mach number effects. The quasi-steady method is discussed in appendix B. This method makes use of steady-state lift distributions determined either experimentally or analytically. Hence, quasi-steady aerodynamic forces are Mach number dependent but only approximate the unsteady effects. References 1 and 19 contain additional information on these and other methods for predicting aerodynamic forces.

Using either method, the aerodynamic forces and moments may be expressed in the form (appendixes A and B)

$$F_{a,y} = C_{n,\alpha}(\alpha + \alpha_w) + C_{n,\dot{\theta}}\dot{\theta} + C_{n,\dot{\alpha}}(\dot{\alpha} + \dot{\alpha}_w) + C_{n,\ddot{\theta}}\ddot{\theta} + \sum_i C_{n,q_i} q_i(t) + \sum_i C_{n,\dot{q}_i}\dot{q}_i(t) + \sum_i C_{n,\ddot{q}_i}\ddot{q}_i(t) \tag{36}$$

$$M_{a,cg} = C_{m,\alpha}(\alpha + \alpha_w) + C_{m,\dot{\theta}}\dot{\theta} + C_{m,\dot{\alpha}}(\dot{\alpha} + \dot{\alpha}_w) + C_{m,\ddot{\theta}}\ddot{\theta} + \sum_i C_{m,q_i} q_i(t) + \sum_i C_{m,\dot{q}_i}\dot{q}_i(t) + \sum_i C_{m,\ddot{q}_i}\ddot{q}_i(t) \tag{37}$$

$$Q_{j,a} = C_{j,\alpha}(\alpha + \alpha_w) + C_{j,\dot{\theta}}\dot{\theta} + C_{j,\dot{\alpha}}(\dot{\alpha} + \dot{\alpha}_w) + C_{j,\ddot{\theta}}\ddot{\theta} + \sum_i C_{j,q_i} q_i(t) + \sum_i C_{j,\dot{q}_i}\dot{q}_i(t) + \sum_i C_{j,\ddot{q}_i}\ddot{q}_i(t) \tag{38}$$

where $\alpha = \theta - \gamma$. An expression for the wind-induced angle of attack α_w is derived in the following section. The generalized aerodynamic coefficients required in equations (36), (37), and (38) are derived in the appendixes cited.

The axial aerodynamic force or drag may be approximated by the expression

$$F_{a,x} = -qS_oC_A(M) \tag{39}$$

where the coefficient C_A is a function of Mach number.

Wind inputs.- Atmospheric winds contribute to the induced aerodynamic loading through two parameters: dynamic pressure and angle of attack. The dynamic pressure q is given by the equation

$$q = \frac{1}{2}\rho V_{m,w}^2 \tag{40}$$

where $V_{m,w}$ is the velocity of the launch vehicle relative to the wind. In the present analysis penetration effects are neglected and $V_{m,w}$ and α_w are defined at the gravity center, that is, $V_{m,w} = V_{m,w}(x_{cg},t)$ and $\alpha_w = \alpha_w(x_{cg}t)$. From the vector diagram illustrated in figure 1, the quantity $V_{m,w}$ may be expressed as follows in terms of the center-of-gravity velocity, wind velocity, and the flight-path angle, by using the law of cosines:

$$V_{m,w} = \sqrt{V_m^2 + V_w^2 + 2V_mV_w \cos\gamma} \tag{41}$$

The magnitude of the center-of-gravity velocity vector is given by the following equation:

$$V_m = \sqrt{V_x^2 + V_y^2} \tag{42}$$

and, in a similar manner, an expression for the rigid-body angle of attack α may be derived.

$$\alpha = \tan^{-1}\left(\frac{-V_y}{V_x}\right) \tag{43}$$

Again from figure 1, the wind-induced angle of attack α_w may be determined by equating the components of $\vec{V}_{m,w}$ and $\vec{V}_w$ which are perpendicular to $\vec{V}_m$ and is given by the following equation:

$$\alpha_w = \sin^{-1}\left(\frac{V_w \sin \gamma}{V_{m,w}}\right) \tag{44}$$

Wind velocity and atmospheric density, pressure, and the velocity of sound vary with altitude. The equation relating altitude to time is

$$h(t) = \int_0^t V_m \sin \gamma \, dt \tag{45}$$

In a similar manner the range, or distance traveled along the horizontal inertial axis (fig. 1), is given by the following equation:

$$r(t) = \int_0^t V_m \cos \gamma \, dt \tag{46}$$

A summary of equations is presented in appendix E.

COMPUTER PROGRAM

General

The launch-vehicle wind-response equations were programed for solution on a high-speed digital computer. This section is devoted to a brief description of the computer routine, its features and scope. An effort was made to keep the program as general as possible in order to accommodate a variety of vehicles. The program has provisions for as many as three bending and two propellant slosh degrees of freedom. Linear aerodynamic coefficients obtained by either momentum theory or the quasi-steady method may be used.

Time-dependent input parameters were approximated by using tabulated data and a linear interpolation subroutine. For the type of vehicles under consideration, table sizes of 10 to 30 discrete time values were found to render satisfactory linear approximations of the time varying parameters. The drag coefficient C_A was defined by a Mach number table of size 40, that is, specified at 40 discrete Mach number conditions. In order to accommodate

detailed wind inputs, the wind velocity V_w was defined by an altitude table of size 1000. For example, with an altitude ceiling of 60,000 feet the wind input V_w may be defined about every 60 feet of altitude although the table may be compressed in certain altitude intervals and expanded in others to provide maximum definition.

Propellant Slosh Considerations

Propellant sloshing, as previously discussed, was simulated with spring mass systems. The slosh parameters (m_k, ξ_k, and x_k) required by this analogy may be determined either from analytical studies or experimental data. The circular slosh frequency ω_k was programed, however, to account for its dependence on the local axial acceleration field. The following equation was utilized in the computer program to generate slosh frequency:

$$\omega_k = \sqrt{\Omega_k a_x} \tag{47}$$

where a_x is an assumed (based on a nominal trajectory) absolute axial acceleration time history. The parameter Ω_k is a function of tank geometry and fluid depth and may be evaluated from information presented in the literature. (See, for example, refs. 1, 11, and 12.)

Aerodynamic Considerations

Reference to appendix B reveals that the integrands in the quasi-steady aerodynamic coefficients are functions of Mach number M and that these integrations should be performed in parallel with the solution of the equations of motion. Such a procedure is unnecessary since the Mach number time history for a wind-disturbed ascent varies little from that computed for a drag inclusive particle trajectory. Thus, if quasi-steady aerodynamics are used, the program requires that a Mach number time relationship be determined or assumed so that the associated integrations required in the linear aerodynamic coefficients may be computed externally. Atmospheric density ρ, pressure p_o, and velocity of sound V_s were obtained from a standard atmosphere. (See ref. 21.)

Bending Moments

The distributed loading exerted on the structure of a launch vehicle may be integrated to yield bending-moment time histories. Such a procedure has been followed in appendix D in order to obtain an equation for the bending moments (eq. (D8)). Provision was included in the computer program for up to 5 bending-moment stations (5 time histories). Integrals required in equation (D8) are submitted in a time table. Either momentum or quasi-steady aerodynamics may be used. For the latter situation, the aerodynamic integrals (appendix D) are

computed externally by means of an assumed Mach number time history as discussed in the preceding section.

Integration Technique

Integration of the nonlinear, time-dependent differential equations was accomplished through the application of an equivalent fifth-order integration by means of a fourth-order Runge-Kutta routine. Salient features of the numerical integration scheme are discussed in this section. The dependent variables, that is, the velocities and displacements, were computed for both a whole and two half intervals and the results compared to establish whether the computing interval should be halved, doubled, or remain unchanged. Furthermore, on the basis of the difference between the whole and two half increment computations, the latter was improved by a correction procedure known as extrapolation to zero interval size (see the discussion entitled "Deferred Approach to the Limit," ref. 22). The correction factor ΔZ is given by the equation

$$\Delta Z = \frac{1}{15}(Z_2 - Z_1) \tag{48}$$

where Z_1 is a particular dependent variable computed on the basis of a whole interval and Z_2 is the same variable established using two half intervals. The correction factor ΔZ is added algebraically to Z_2 in order to obtain the equivalent fifth-order approximation of the dependent variable.

The computing interval adjustment criteria was based on the relative error. The following approximation of the relative error was used in the integration routine:

$$\text{Relative error} = \frac{|Z_2 - Z_1|}{15|Z_2|} \tag{49}$$

Computing Interval Adjustment Criteria

(1) If the relative error is greater than its respective maximum allowable error the computing interval is halved and the calculation repeated.

(2) If the relative error is less than 1 percent of its maximum allowable error the computation is accepted, but the interval is doubled for the next computation.

(3) If neither conditions (1) or (2) are satisfied the computing interval remains unchanged.

(4) If the absolute value of a particular dependent variable is less than 10^{-5} halving will not be initiated as a result of this variable satisfying condition (1) nor will doubling be allowed if all other variables satisfy condition (2).

(5) Halving criteria for any one dependent variable requires halving for all, but all variables must satisfy the doubling criteria before the computing interval is doubled.

A maximum allowable error of 10^{-4} was employed in the program for all dependent variables and the "read-in" or initial computing interval was set at 10^{-3} seconds. Partial double precision internal addition (ref. 23) was used to minimize round-off error. Since the equations are linearly cross-coupled through the accelerations, a matrix inversion was employed to determine the acceleration values.

APPLICATION AND RESULTS

Configuration

In order to illustrate the procedure, the response of a typical launch vehicle was computed. A preliminary design configuration of a booster system, which has a thrust-weight ratio of approximately 1.25 at launch, was chosen as the example launch vehicle.

Mass and stiffness properties.- Structural deformation of the vehicle's center line was represented by the superposition of the first three free-free simple beam modes. The mode shapes and frequencies shown in figure 4 were computed by using the mass and stiffness properties for a flight time of $t = 62$ seconds and are indicative of the relative shapes occurring at other times. The modes are normalized to unity at the gimbal station, that is, $\phi_i(0) = 1.0$ for $i = 1, 2,$ and 3. The analysis included two slosh degrees of freedom representing the fundamental modes of the first-stage liquid-oxygen and fuel tanks, respectively. The frequencies of the two slosh systems 62 seconds after launch are about 4.7 radians/sec.

Aerodynamics.- Aerodynamic data available for the example vehicle consisted of total normal-force and pitching-moment coefficient $C_{N_\alpha}(M)$ and $C_{m_\alpha}(M)$ as presented in figure 5. Shown also in this figure is the axial force or drag coefficient $C_A(M)$. For illustrative purposes a normal aerodynamic lift distribution was assumed in the form shown in figure 6 and the parameters C_1 and C_2 determined so that the assumed distribution produced the same $C_{N_\alpha}(M)$ and $C_{m_\alpha}(M)$ for a given Mach number. The afterbody lift was approximated by an exponential variation; the forebody lift was assumed linear. As has been previously explained, it is expedient to assume an explicit Mach number time relationship so that the integrations associated with the quasi-steady coefficients may be computed externally. The assumed Mach number time variation is shown in figure 5.

Control system.- The control system and gimbaled engine equations for the example launch vehicle have been previously discussed. The vehicle, however, was flown without angle-of-attack feedback ($\mu_2 = 0$). Ascent of the vehicle was

autopilot controlled, rising vertically for the first 15 seconds of flight and then executing a slow pitch-over maneuver. The pitch program θ_c approximates a no-wind, zero-lift trajectory and is illustrated in figure 7.

Wind profile.- A measured wind profile obtained by the smoke-trail method (ref. 6) was used as input. The profile is shown in figure 8 and has a maximum wind velocity of approximately 300 feet per second. The wind was assumed to increase linearly from zero velocity at launch to the first smoke-trail data point and to decrease linearly from the last data point to zero velocity at 60,000 feet. The wind input was defined in a table that specified V_w at approximately every 82 feet (25 meters) of altitude. It should be noted that V_w was used as a tailwind.

Launch-Vehicle Response and Bending Loads

The example launch vehicle was flown through the measured wind profile illustrated in figure 8. A brief summary of the resulting response and induced wind loads is presented in this section.

Trajectory.- Mach number and dynamic pressure time histories for the wind disturbed ascent trajectory are shown in figure 9(a). The vehicle experiences a maximum dynamic pressure of 790 lb/sq ft about 82 seconds after lift-off. The Mach number at this time is approximately 2.0. Because the quasi-steady aerodynamic coefficients were computed externally and related to time by means of an expected or assumed Mach number time relationship, it is of interest to check the validity of this computational simplification. A comparison of the computed and assumed Mach numbers is also shown in figure 9(a). The figure indicates that, due to atmospheric winds, the assumed Mach number differs slightly from that actually experienced by the vehicle. Figure 9(b) compares the attitude θ and the command attitude θ_c. As a result of the wind, a maximum deviation of about 3° occurs about 77.5 seconds after launch. Also shown is the resulting angle of attack $\alpha + \alpha_w$ and altitude time histories. The vehicle experiences a peak angle of attack of about -6.7° 26 seconds after lift-off due to the pitch-over maneuver. Just prior to penetrating the large shear layer, the magnitude of the angle of attack has decreased to approximately -4.2° ($t = 71.5$ seconds). After passing through the wind shear reversal occurring near an altitude of 36,000 feet (fig. 8), the angle of attack further increases to 3.8° ($t = 77.5$ seconds) which represents the maximum positive excursion. The product of dynamic pressure and angle of attack, that is, $q(\alpha + \alpha_w)$, which is sometimes used as a measure of loads, has a maximum value of approximately $2,950^\circ$-lb/sq ft about 77.5 seconds after launch.

Gimbaled engine, bending mode, and slosh responses.- The response of the gimbaled engine is presented in figure 10. A maximum positive angular displacement of about 3.9° was required. The engine kick at $t = 15$ seconds which starts the vehicle into the pitch program (fig. 7) is apparent as well as the swiveling between 45 and 70 seconds required for control while maneuvering through the smaller wind shear reversals between 10,000 and 30,000 feet.

Passage of the launch vehicle through the larger shear reversal near 36,000 feet required a negative engine rotation (gimbal angle) of about -5.8°.

The response of the three bending modes is illustrated in figure 11, which shows the time histories of the associated generalized coordinates $q_i(t)$ for $i = 1$, 2, and 3. Oscillations at the modal frequencies are negligible, due to relatively smooth wind profile. Since the modes are normalized to unity at the gimbal the results of this figure indicate a maximum first mode deflection at the gimbal point ($x = 0$) of about 0.13 foot. The nose deflection at $x = L$ would be about $3\frac{1}{2}$ times larger in the first mode as is apparent from the information presented in figure 4. The actual deflection $u(x,t)$ of any point on the structural center line can be obtained by superposition of the three modes. For example, if equation (1) and the results of figure 4 are used, the total nose deflection occurring at a flight time of 62 seconds can be computed as follows:

$$u(x=L,t=62) = 3.4(-0.048) + (-10.4)(0.10)(10)^{-2} + 6.1(-0.18)(10)^{-2} = -0.184 \text{ ft}$$

The responses of the two slosh masses are illustrated in figure 12. It should be noted that the subscripts 1 and 2 refer to the first-stage fuel and liquid-oxygen tanks, respectively. Maximum displacements of the spring mass systems are less than ± 0.42 foot. Because of the small amounts of damping associated with these degrees of freedom, the responses are oscillatory.

Bending moments.- The bending moments produced at five longitudinal stations along the structural center line were computed. The time histories are presented in figure 13. Peak negative bending moments occur about 71.5 seconds after launch. Maximum positive bending moments occur a few seconds later at approximately 77.5 seconds as a result of the vehicle recovering from the large wind shear reversal near an altitude of 36,000 feet. A maximum bending moment of about 0.59×10^6 ft-lb was produced at station $x_{b,2} = 33.32$ feet. A distribution of the bending moments for this time ($t = 77.5$ seconds), cross-plotted from figure 13, is presented in figure 14.

CONCLUDING REMARKS

An analytical procedure has been developed for computing the motions and bending moments experienced by a flexible launch vehicle during ascent through atmospheric winds. The method is particularly suitable for use with detailed wind inputs, such as those obtained by smoke-trail observations, which describe the combined amplitude, shear, and gust characteristics of the atmospheric wind environment.

The nonlinear differential equations of motions, which have time-dependent coefficients, were programed for solution on a high-speed digital computer. As

an illustrative example, the motions and bending moments were computed for a typical launch vehicle ascending through a smoke-trail wind velocity profile.

Langley Research Center,
National Aeronautics and Space Administration,
Langley Station, Hampton, Va., June 30, 1964.

APPENDIX A

SLENDER-BODY MOMENTUM AERODYNAMICS

In accordance with momentum theory (as discussed in ref. 19) the lift per unit length $l(x,t)$ developed on a slender body is given by the expression

$$l(x,t) = -\rho\left(V_{m,w}\frac{\partial}{\partial x} - \frac{\partial}{\partial t}\right)\left[S(x)\ w(x,t)\right] \tag{A1}$$

where $S(x)$ is the local cross-sectional area of revolution and $w(x,t)$ is the local time-dependent downwash. From coordinate system considerations (as illustrated in fig. 1) the downwash may be written as follows (neglecting $\dot{x}_{cg}$):

$$w(x,t) = V_{m,w}\left[\alpha_w + (\theta - \gamma) + \sum_i \phi_i'(x)\ q_i(t)\right] - \dot{\theta}(x - x_{cg}) - \sum_i \phi_i(x)\ \dot{q}_i(t) \tag{A2}$$

where $V_{m,w}$ is the velocity of the launch vehicle relative to the wind. Using this expression for downwash, the lift per unit length may be expanded to the form:

$$\begin{aligned} l(x,t) = {} & -\rho V_{m,w}^2 S'(x)\left[(\theta - \gamma) + \alpha_w\right] - \rho V_{m,w}^2 S'(x) \sum_i \phi_i'(x)\ q_i(t) + \rho V_{m,w} S'(x)(x - x_{cg})\dot{\theta} + \rho V_{m,w} S'(x) \sum_i \phi_i(x)\ \dot{q}_i(t) \\ & - \rho V_{m,w}^2 S(x) \sum_i \phi_i''(x)\ q_i(t) + \rho V_{m,w} S(x)\dot{\theta} + 2\rho V_{m,w} S(x) \sum_i \phi_i'(x)\ \dot{q}_i(t) + \rho \dot{V}_{m,w} S(x)\left[(\theta - \gamma) + \alpha_w\right] \\ & + \rho \dot{V}_{m,w} S(x) \sum_i \phi_i'(x)\ q_i(t) + \rho V_{m,w} S(x)\left[(\dot{\theta} - \dot{\gamma}) + \dot{\alpha}_w\right] - \rho\ddot{\theta}(x - x_{cg}) S(x) - \rho S(x) \sum_i \phi_i(x)\ \ddot{q}_i(t) \end{aligned} \tag{A3}$$

The resultant normal force, pitching moment, and jth generalized force may be obtained by integrating the distribution over the length in accordance with the following three equations:

$$\left.\begin{aligned} F_{a,y} &= \int_0^L l(x,t)\ dx \\ M_{a,cg} &= \int_0^L (x - x_{cg})\, l(x,t)\ dx \\ Q_{j,a} &= \int_0^L \phi_j(x)\ l(x,t)\ dx \end{aligned}\right\} \tag{A4}$$

If penetration effects are neglected, by defining $V_{m,w} = V_{m,w}(x_{cg},t)$ and $\alpha_w = \alpha_w(x_{cg},t)$, the coefficients required in equations (36), (37), and (38) may be determined as follows:

$$C_{n,\alpha} = \rho S_o\left[-V_{m,w}^2 \int_0^L \frac{S'(x)}{S_o}\,dx + \dot{V}_{m,w} \int_0^L \frac{S(x)}{S_o}\,dx\right]$$

$$C_{n,\dot{\theta}} = \rho S_o V_{m,w}\left[\int_0^L (x - x_{cg}) \frac{S'(x)}{S_o}\,dx + \int_0^L \frac{S(x)}{S_o}\,dx\right]$$

$$C_{n,\dot{\alpha}} = \rho S_o V_{m,w}\left[\int_0^L \frac{S(x)}{S_o}\,dx\right]$$

$$C_{n,\ddot{\theta}} = \rho S_o\left[-\int_0^L (x - x_{cg}) \frac{S(x)}{S_o}\,dx\right]$$

$$C_{n,q_i} = \rho S_o\left[-V_{m,w}^2 \int_0^L \frac{S'(x)}{S_o} \phi_i'(x)\,dx - V_{m,w}^2 \int_0^L \frac{S(x)}{S_o} \phi_i''(x)\,dx + \dot{V}_{m,w} \int_0^L \frac{S(x)}{S_o} \phi_i'(x)\,dx\right]$$

$$C_{n,\dot{q}_i} = \rho S_o V_{m,w}\left[\int_0^L \frac{S'(x)}{S_o} \phi_i(x)\,dx + 2\int_0^L \frac{S(x)}{S_o} \phi_i'(x)\,dx\right]$$

$$C_{n,\ddot{q}_i} = \rho S_o\left[-\int_0^L \frac{S(x)}{S_o} \phi_i(x)\,dx\right]$$

$$C_{m,\alpha} = \rho S_o\left[-V_{m,w}^2 \int_0^L (x - x_{cg}) \frac{S'(x)}{S_o}\,dx + \dot{V}_{m,w} \int_0^L (x - x_{cg}) \frac{S(x)}{S_o}\,dx\right]$$

$$C_{m,\dot{\theta}} = \rho S_o V_{m,w}\left[\int_0^L (x - x_{cg})^2 \frac{S'(x)}{S_o}\,dx + \int_0^L (x - x_{cg}) \frac{S(x)}{S_o}\,dx\right]$$

$$C_{m,\dot{\alpha}} = \rho S_o V_{m,w}\left[\int_0^L (x - x_{cg}) \frac{S(x)}{S_o}\,dx\right]$$

$$C_{m,\ddot{\theta}} = \rho S_o \left[-\int_0^L (x - x_{cg})^2 \frac{S(x)}{S_o} \, dx \right]$$

$$C_{m,q_i} = \rho S_o \left[-V_{m,w}^2 \int_0^L (x - x_{cg}) \frac{S'(x)}{S_o} \phi_i'(x) \, dx \right.$$
$$\left. - V_{m,w}^2 \int_0^L (x - x_{cg}) \frac{S(x)}{S_o} \phi_i''(x) \, dx + \dot{V}_{m,w} \int_0^L (x - x_{cg}) \frac{S(x)}{S_o} \phi_i'(x) \, dx \right]$$

$$C_{m,\dot{q}_i} = \rho S_o V_{m,w} \left[\int_0^L (x - x_{cg}) \frac{S'(x)}{S_o} \phi_i(x) \, dx + 2 \int_0^L (x - x_{cg}) \frac{S(x)}{S_o} \phi_i'(x) \, dx \right]$$

$$C_{m,\ddot{q}_i} = \rho S_o \left[-\int_0^L (x - x_{cg}) \frac{S(x)}{S_o} \phi_i(x) \, dx \right]$$

$$C_{j,\alpha} = \rho S_o \left[-V_{m,w}^2 \int_0^L \frac{S'(x)}{S_o} \phi_j(x) \, dx + \dot{V}_{m,w} \int_0^L \frac{S(x)}{S_o} \phi_j(x) \, dx \right]$$

$$C_{j,\dot{\theta}} = \rho S_o V_{m,w} \left[\int_0^L (x - x_{cg}) \frac{S'(x)}{S_o} \phi_j(x) \, dx + \int_0^L \frac{S(x)}{S_o} \phi_j(x) \, dx \right]$$

$$C_{j,\dot{\alpha}} = \rho S_o V_{m,w} \left[\int_0^L \frac{S(x)}{S_o} \phi_j(x) \, dx \right]$$

$$C_{j,\ddot{\theta}} = \rho S_o \left[-\int_0^L (x - x_{cg}) \frac{S(x)}{S_o} \phi_j(x) \, dx \right]$$

$$C_{j,q_i} = \rho S_o \left[-V_{m,w}^2 \int_0^L \frac{S'(x)}{S_o} \phi_j(x) \phi_i'(x) \, dx \right.$$
$$\left. - V_{m,w}^2 \int_0^L \frac{S(x)}{S_o} \phi_j(x) \phi_i''(x) \, dx + \dot{V}_{m,w} \int_0^L \frac{S(x)}{S_o} \phi_j(x) \phi_i'(x) \, dx \right]$$

$$C_{j,\dot{q}_i} = \rho S_o V_{m,w} \left[\int_0^L \frac{S'(x)}{S_o} \phi_j(x) \phi_i(x) \, dx + 2 \int_0^L \frac{S(x)}{S_o} \phi_j(x) \phi_i'(x) \, dx \right]$$

$$C_{j,\ddot{q}_i} = \rho S_o \left[-\int_0^L \frac{S(x)}{S_o} \phi_j(x) \phi_i(x) \, dx \right]$$

APPENDIX B

QUASI-STEADY AERODYNAMICS

Mach number effects can be accounted for through the use of a quasi-steady type of aerodynamic analysis (ref. 1). With this approach, the normal aerodynamic force per unit length may be written as:

$$l(x,t) = qS_o \, c_{n_\alpha}(x,M) \, \frac{w(x,t)}{V_{m,w}} \tag{B1}$$

where $c_{n_\alpha}(x,M)$ is the slope of the local normal-force coefficient and q is the dynamic pressure. For the present analysis $c_{n_\alpha}(x,M)$ is assumed independent of angle of attack and is thus only a function of the running coordinate x and the Mach number M. The downwash $w(x,t)$ is given by equation (A2) and $V_{m,w}$ is given by equation (41). After substituting for the downwash, the normal-force distribution (eq. (B1)) may be expanded to the following form:

$$l(x,t) = qS_o \, c_{n_\alpha}(x,M)\left\{\alpha + \alpha_w + \sum_i \phi_i'(x) \, q_i(t) - \frac{1}{V_{m,w}}\left[\dot{\theta}\left(x - x_{cg}\right) + \sum_i \phi_i(x) \, \dot{q}_i(t)\right]\right\} \tag{B2}$$

where $\alpha = \theta - \gamma$.

The normal force, pitching moment, and generalized aerodynamic force for the jth bending mode may be obtained from equation (A4). If penetration effects are neglected, as was done previously in appendix A, the quasi-steady aerodynamic coefficients required in equations (36), (37), and (38) may be established as follows:

$$C_{n,\alpha} = qS_o \int_0^L c_{n_\alpha}(x,M) \, dx$$

$$C_{n,\dot{\theta}} = -\frac{qS_o}{V_{m,w}} \int_0^L \left(x - x_{cg}\right) c_{n_\alpha}(x,M) \, dx$$

$$C_{n,\dot{\alpha}} = 0$$

$$C_{n,\ddot{\theta}} = 0$$

$$C_{n,q_i} = qS_o \int_0^L \phi_i'(x) \, c_{n_\alpha}(x,M) \, dx$$

$$C_{n,\dot{q}_i} = - \frac{qS_o}{V_{m,w}} \int_0^L \phi_i(x)\ c_{n_\alpha}(x,M)\ dx$$

$$C_{n,\ddot{q}_i} = 0$$

$$C_{m,\alpha} = qS_o \int_0^L \left(x - x_{cg}\right) c_{n_\alpha}(x,M)\ dx$$

$$C_{m,\dot{\theta}} = - \frac{qS_o}{V_{m,w}} \int_0^L \left(x - x_{cg}\right)^2 c_{n_\alpha}(x,M)\ dx$$

$$C_{m,\dot{\alpha}} = 0$$

$$C_{m,\ddot{\theta}} = 0$$

$$C_{m,q_i} = qS_o \int_0^L \left(x - x_{cg}\right) \phi_i'(x)\ c_{n_\alpha}(x,M)\ dx$$

$$C_{m,\dot{q}_i} = - \frac{qS_o}{V_{m,w}} \int_0^L \left(x - x_{cg}\right) \phi_i(x)\ c_{n_\alpha}(x,M)\ dx$$

$$C_{m,\ddot{q}_i} = 0$$

$$C_{j,\alpha} = qS_o \int_0^L \phi_j(x)\ c_{n_\alpha}(x,M)\ dx$$

$$C_{j,\dot{\theta}} = - \frac{qS_o}{V_{m,w}} \int_0^L \left(x - x_{cg}\right) \phi_j(x)\ c_{n_\alpha}(x,M)\ dx$$

$$C_{j,\dot{\alpha}} = 0$$

$$C_{j,\ddot{\theta}} = 0$$

$$C_{j,q_i} = qS_o \int_0^L \phi_j(x)\ \phi_i'(x)\ c_{n_\alpha}(x,M)\ dx$$

$$C_{j,\dot{q}_i} = - \frac{qS_o}{V_{m,w}} \int_0^L \phi_j(x)\ \phi_i(x)\ c_{n_\alpha}(x,M)\ dx$$

$$C_{j,\ddot{q}_i} = 0$$

APPENDIX C

PROPULSIVE FORCES AND PROPELLANT FLOW EFFECTS

Equations for the propulsive forces and moments, including propellant flow effects, are derived in this appendix. The launch vehicle is assumed to have a single rocket-engine thrust chamber which swivels to produce the necessary control forces. The more general case involving both gimbaled and nongimbaled engines serves only to complicate the analysis and is unnecessary since the forces and moments associated with the latter may be obtained by specializing the results of the former. In the subsequent development the following symbols, not previously defined, are used:

A cross-sectional area of thrust chamber exit, sq ft

d perpendicular distance from gimbal point to nozzle exit face, ft

$K(x,t)$ rate of mass flow through a section at coordinate x, $\int_x^L \frac{\partial m(\lambda,t)}{\partial t}\, d\lambda$, $\frac{\text{lb-sec}}{\text{ft}}$

M_δ propulsive moment about gimbal exerted on engine thrust chamber, ft-lb

p_e pressure at thrust chamber exit face (exhaust condition), lb/sq ft

$V(x,t)$ average velocity at which propellant mass is being transferred across a section located at coordinate x, ft/sec

$V(\eta,t)$ average velocity at which mass (exhaust gases) is being transferred across a section in thrust chamber at coordinate η

V_e velocity of exhaust gases at exit from thrust chamber, $v(\eta=d,t)$, ft/sec

$V_o = V(0,t)$ ft/sec

w rate at which total mass of launch vehicle is changing, negative for systems losing mass, $K(0,t)$, $\frac{\text{lb-sec}}{\text{ft}}$

$w_x(x,t)$, $w_y(x,t)$ x- and y-components of distributed loading exerted on a launch-vehicle structure by internal propellant flow, lb/ft

$w_{e,x}(\eta,t)$, $w_{e,y}(\eta,t)$ x- and y-components of distributed loading exerted on gimbaled thrust chamber by flow of exhaust gases, lb/ft

$\Delta(\eta-d)$ delta function

λ dummy variable for x, ft

The force (per unit length) exerted on a launch-vehicle structure by the local propellant mass transfer may be obtained from the information available in reference 7. The results presented therein are obtained from momentum considerations and are easily modified to include a gimbaled thrust chamber (engine) and a modal representation for structural deformations. When such an extension is made and the results transformed from an inertial (space-fixed) reference frame, as used in reference 7, to the rotating body frame used herein (fig. 1) the x- and y-components of the distributed loading are found to be as follows:

$$w_x(x,t) = -\frac{\partial}{\partial x}\left\{K(x,t)\left[-V(x,t) + V_x - \dot{x}_{cg} - \dot{\theta}\sum_i \phi_i(x)\, q_i(t)\right]\right\} \tag{C1}$$

$$w_y(x,t) = -\frac{\partial}{\partial x}\left\{K(x,t)\left[-V(x,t)\sum_i \phi_i'(x)\, q_i(t) + V_y + (x - x_{cg})\dot{\theta} + \sum_i \phi_i(x)\, \dot{q}_i(t)\right]\right\} \tag{C2}$$

where $V(x,t)$ is the average (over the cross section) velocity at which propellant mass is being transferred across the section at coordinate x. It should be noted that $V(x,t)$ is tangent to the deformed structural center line and is positive in the direction of flow - that is, toward the origin $x = 0$. The quantity $K(x,t)$ represents the rate at which propellant mass is being transferred across a section located at coordinate x and has the following definition:

$$K(x,t) = \int_x^L \frac{\partial m(\lambda,t)}{dt}\, d\lambda \tag{C3}$$

It is apparent from equation (C3) that $K(L,t) = 0$ whereas $K(0,t) = w$; that is, the rate of mass flow at the gimbal point (into the thrust chamber) is w and represents the rate at which the total mass of the launch vehicle is changing. It should be noted that w is a negative quantity.

Along the longitudinal axis of the gimbaled engine nozzle the mass-flow rate is constant and equals w. The velocity $V(\eta,t)$, however, undergoes a pronounced change as the flow (exhaust gases) is expanded to the exit condition at $\eta = d$. In addition, there is a force exerted on the thrust chamber due to the difference between atmospheric pressure p_o and the pressure of the exhaust gases at exit p_e. The pressure force $-A(p_e - p_o)$ is included by means of a delta function $\Delta(\eta-d)$, where it is assumed that the exhaust pressure is

uniformly distributed over the exit face. Hence, the x- and y-components of the loading per unit length along the nozzle may be determined in a similar manner and are given by the following two equations:

$$w_{e,x}(\eta,t) = -w \frac{\partial}{\partial \eta} \left\{ -V(\eta,t) + V_x - \dot{x}_{cg} - \dot{\theta} \sum_i \phi_i(0)\, q_i(t) - \eta\dot{\theta}\left[\delta - \sum_i \phi_i'(0)\, q_i(t)\right] + \eta\left[\delta - \sum_i \phi_i'(0)\, q_i(t)\right]\left[\dot{\delta} - \sum_i \phi_i(0)\, \dot{q}_i(t)\right] \right\} + A\left(p_e - p_o\right) \Delta(\eta - d) \tag{C4}$$

$$w_{e,y}(\eta,t) = -w \frac{\partial}{\partial \eta} \left\{ V(\eta,t)\left[\delta - \sum_i \phi_i'(0)\, q_i(t)\right] + V_y - \left(x_{cg} + \eta\right)\dot{\theta} + \sum_i \phi_i(0)\, \dot{q}_i(t) + \eta\left[\dot{\delta} - \sum_i \phi_i'(0)\, \dot{q}_i(t)\right] \right\}$$

$$- A\left(p_e - p_o\right)\left[\delta - \sum_i \phi_i'(0)\, q_i(t)\right] \Delta(\eta - d) \tag{C5}$$

It should be noted that η represents a running coordinate along the longitudinal axis of the thrust chamber as measured from the gimbal point with a positive sense in the direction of flow, that is, in the same direction as $V(\eta,t)$.

With the results of equations (C1) to (C5), it is possible to compute the resulting forces and moments produced by the flowing propellants. The x-component F_x of the total force exerted on the launch vehicle by virtue of the propellant flow may be obtained by integrating the x-component of the distributed loading. Therefore,

$$F_{p,x} = \int_0^L w_x(x,t)\, dx + \int_d^0 w_{e,x}(\eta,t)\, d\eta \tag{C6}$$

When the results of equations (C1), (C3), and (C4) are substituted into equation (C6) and the integration performed, the following equation results:

$$F_{p,x} = \left[-wV_e + A\left(p_e - p_o\right)\right] + w\left(V_x - \dot{x}_{cg}\right) - w\dot{\theta} \sum_i \phi_i(0)\, q_i(t) - wd\dot{\theta}\left[\delta - \sum_i \phi_i'(0)\, q_i(t)\right]$$

$$+ wd\left[\delta - \sum_i \phi_i'(0)\, q_i(t)\right]\left[\dot{\delta} - \sum_i \phi_i'(0)\, \dot{q}_i(t)\right] \tag{C7}$$

In a similar manner the y-component F_y is given by the equation

$$F_{p,y} = \int_0^L w_y(x,t)\, dx + \int_d^0 w_{e,y}(\eta,t)\, d\eta \tag{C8}$$

With the aid of equations (C2), (C3), and (C5), equation (C8) reduces to the following form:

$$F_{p,y} = -\left[-wV_e + A(p_e - p_o)\right]\left[\delta - \sum_i \phi_i'(0)\, q_i(t)\right] + wV_y - wV(0,t)\delta - w(x_{cg} + d)\dot{\theta} + w\sum_i \phi_i(0)\,\dot{q}_i(t) + w\,d\left[\dot{\delta} - \sum_i \phi_i'(0)\,\dot{q}_i(t)\right] \quad (C9)$$

If the distributed loadings (eqs. (C1), (C2), (C4), and (C5)) are multiplied by the proper weighting functions and integrated, the propulsive pitching moment M_p, jth generalized force $Q_{j,p}$, and gimbaled engine moment M_δ may be obtained. For example, the moment M_p produced about the center of gravity by the propellant flow is given by the following expression:

$$M_p = \sum_i \left[-\int_0^L w_x(x,t)\,\phi_i(x)\,dx\right] q_i(t) + \int_0^L (x - x_{cg})\,w_y(x,t)\,dx - \left[\delta - \sum_i \phi_i'(0)\,q_i(t)\right]\int_d^0 \eta w_{e,x}(\eta,t)\,d\eta$$
$$- \int_d^0 (x_{cg} + \eta)\,w_{e,y}(\eta,t)\,d\eta - \sum_i \phi_i(0)\,q_i(t)\int_d^0 w_{e,x}(\eta,t)\,d\eta \quad (C10)$$

When the necessary substitutions are made and the integrations performed, equation (C10) reduces to the following form:

$$M_p = x_{cg}\left[-wV_e + A(p_e - p_o)\right]\left[\delta - \sum_i \phi_i'(0)\,q_i(t)\right] - \left[-wV_e + A(p_e - p_o)\right]\sum_i \phi_i(0)\,q_i(t) + w\dot{\theta}(x_{cg} + d)^2 - w(x_{cg} + d)\sum_i \phi_i(0)\,\dot{q}_i(t)$$
$$- wd(x_{cg} + d)\left[\dot{\delta} - \sum_i \phi_i'(0)\,\dot{q}_i(t)\right] + wx_{cg}V_o\delta - wx_{cg}V_y + wd\sum_i \phi_i(0)\,\dot{q}_i(t) - w(V_x - \dot{x}_{cg})\sum_i \phi_i(0)\,q_i(t) + w\dot{\theta}\left[\sum_i \phi_i(0)\,q_i(t)\right]^2$$
$$+ wd\dot{\theta}\left[\delta - \sum_i \phi_i'(0)\,q_i(t)\right]\sum_j \phi_j(0)\,q_j(t) - wd\left[\delta - \sum_i \phi_i'(0)\,q_i(t)\right]\left[\dot{\delta} - \sum_j \phi_j'(0)\,\dot{q}_j(t)\right]\sum_j \phi_j(0)\,q_j(t)$$
$$+ \tfrac{1}{2}w\dot{\theta}d^2\left[\delta - \sum_i \phi_i'(0)\,q_i(t)\right]^2 - \tfrac{1}{2}wd^2\left[\dot{\delta} - \sum_i \phi_i'(0)\,\dot{q}_i(t)\right]\left[\delta - \sum_j \phi_j'(0)\,q_j(t)\right]^2 - wx_{cg}d\dot{\theta} - \tfrac{1}{2}wd^2\dot{\theta}$$
$$+ \tfrac{1}{2}wd^2\left[\dot{\delta} - \sum_i \phi_i'(0)\,\dot{q}_i(t)\right] + c_p \quad (C11)$$

where

$$c_p = \int_0^L K(x,t)\left[-V(x,t)\sum_i \phi_i'(x)\,q_i(t) + V_y + (x - x_{cg})\dot{\theta} + \sum_i \phi_i(x)\,\dot{q}_i(t)\right]dx - \sum_i \left\{\int_0^L K(x,t)\,\phi_i'(x)\left[-V(x,t) + (V_x - \dot{x}_{cg})\right.\right.$$
$$\left.\left. - \dot{\theta}\sum_j \phi_j(x)\,q_j(t)\right]dx\right\} q_i(t) \quad (C12)$$

The generalized force associated with the jth bending mode due to the flowing propellants is obtained in a similar manner and is given by the following equation:

$$Q_{j,p} = \int_0^L \phi_j(x)\,w_y(x,t)\,dx + \int_d^0 \left[\phi_j(0) - \eta\phi_j'(0)\right] w_{e,y}(\eta,t)\,d\eta - \int_d^0 \eta\phi_j'(0)\left[\delta - \sum_i \phi_i'(0)\,q_i(t)\right] w_{e,x}(\eta,t)\,d\eta \quad (C13)$$

which reduces to the form

$$Q_{j,p} = w\phi_j(0)V_y - \phi_j(0)\left[-wV_e + A(p_e - p_o)\right]\left[\delta - \sum_i \phi_i'(0)\, q_i(t)\right] - w\phi_j(0)(x_{cg} + d)\dot{\theta} + w\phi_j(0) \sum_i \phi_i(0)\, \dot{q}_i(t)$$

$$+ wd\phi_j(0)\left[\dot{\delta} - \sum_i \phi_i'(0)\, \dot{q}_i(t)\right] - w\phi_j(0)V_o\delta + \frac{1}{2}\, wd^2\phi_j'(0)\dot{\theta} - \frac{1}{2}\, wd^2\phi_j'(0)\left[\dot{\delta} - \sum_i \phi_i'(0)\, \dot{q}_i(t)\right]$$

$$+ \frac{1}{2}\, w\dot{\theta}d^2\phi_j'(0)\left[\delta - \sum_i \phi_i'(0)\, q_i(t)\right]^2 - \frac{1}{2}\, wd^2\phi_j'(0)\left[\delta - \sum_i \phi_i'(0)\, q_i(t)\right]^2\left[\dot{\delta} - \sum_j \phi_j'(0)\, \dot{q}_j(t)\right] + c_{jp} \qquad (C14)$$

where

$$c_{j,p} = \int_0^L K(x,t)\, \phi_j'(x)\left[-V(x,t) \sum_i \phi_i'(x)\, q_i(t) + V_y + (x - x_{cg})\dot{\theta} + \sum_i \phi_i(x)\, \dot{q}_i(t)\right] dx \qquad (C15)$$

Finally, the moment about the gimbal exerted on the swiveling engine by the exhaust gases is given by

$$M_\delta = \int_d^0 \eta w_{e,y}(\eta,t)\, d\eta + \int_d^0 \eta\left[\delta - \sum_i \phi_i'(0)\, q_i(t)\right] w_{e,x}(\eta,t)\, d\eta \qquad (C16)$$

which integrates to

$$M_\delta = \frac{1}{2}\, wd^2\left\{\left[\dot{\delta} - \sum_i \phi_i'(0)\, \dot{q}_i(t)\right] - \dot{\theta}\right\} + \frac{1}{2}\, wd^2\left[\delta - \sum_i \phi_i'(0)\, q_i(t)\right]^2\left\{\left[\dot{\delta} - \sum_i \phi_i'(0)\, \dot{q}_i(t)\right] - \dot{\theta}\right\} \qquad (C17)$$

APPENDIX D

BENDING MOMENTS

The bending moment acting at any point along the structure of a booster vehicle is determined by the loads summation method as discussed in reference 8. Application of the method requires finding the lateral load per unit length and integrating to find the resultant bending moment. The loading may be conveniently divided into four types: inertial, slosh, aerodynamic, and gravity.

The inertial loading requires knowledge of the acceleration vector of a point on the vehicle structural center line. This vector is obtained by differentiating the velocity vector $\vec{V}_p$, as given by equation (4). Thus,

$$\dot{\vec{V}}_p = \frac{\partial \vec{V}_p}{\partial t} + \dot{\theta}\left(\vec{k} \times \vec{V}_p\right) \tag{D1}$$

where the unit vector $\vec{k}$ is formed from the cross product $\vec{i} \times \vec{j}$. Equation (D1) expands to the following form:

$$\dot{\vec{V}}_p = \vec{i}\left[\left(\dot{V}_x - \ddot{x}_{cg}\right) - 2\dot{\theta}\sum_i \phi_i(x)\,\dot{q}_i(t) - \ddot{\theta}\sum_i \phi_i(x)\,q_i(t) - V_y\dot{\theta} - \left(x - x_{cg}\right)\dot{\theta}^2\right] + \vec{j}\left[\dot{V}_y + \left(x - x_{cg}\right)\ddot{\theta} + \sum_i \phi_i(x)\,\ddot{q}_i(t) + \left(V_x - 2\dot{x}_{cg}\right)\dot{\theta} - \dot{\theta}^2\sum_i \phi_i(x)\,q_i(t)\right] \tag{D2}$$

Only the y-component of the acceleration vector $\dot{\vec{V}}_p$ contributes to the lateral inertial loading (less slosh) l_I. In accordance with d'Alembert's principle, this quantity is given by the following equation:

$$l_I(x,t) = -m(x,t)\left[\dot{V}_y + \left(x - x_{cg}\right)\ddot{\theta} + \sum_i \phi_i(x)\,\ddot{q}_i(t) + \left(V_x - 2\dot{x}_{cg}\right)\dot{\theta} - \dot{\theta}^2\sum_i \phi_i(x)\,q_i(t)\right] \tag{D3}$$

The slosh masses also contributed to the inertial loading. However, inclusion of the slosh contributions in the bending-moment expression is simplified if the spring and viscous damping forces are considered. Using this approach, each slosh mass produces a concentrated force F_k at its attachment point, which is

$$F_k = m_k\omega_k^2\lambda_k + 2m_k\omega_k\xi_k\dot{\lambda}_k \tag{D4}$$

The gravity loading per unit length is given by the following equation:

$$l_g(x,t) = -m(x,t)g\cos\theta \tag{D5}$$

The distributed aerodynamic loading $l(x,t)$ is given by either equation (A3) or (B1).

The bending moment produced at any station located by the coordinate $x = x_{b,n}$ is determined by integrating the total lateral loading in the following manner:

$$M_{b,n} = \int_{x_{b,n}}^{L} \left(x - x_{b,n}\right)\left(l_I + l_g + l\right) dx + \sum_k U\left(x_k - x_{b,n}\right)\left(x_k - x_{b,n}\right)F_k \qquad (D6)$$

where $U\left(x_k - x_{b,n}\right)$ is the unit step function and has the following definition:

$$\left.\begin{aligned} U\left(x_k - x_{b,n}\right) &= 0 \qquad \left(x_k < x_{b,n}\right) \\ U\left(x_k - x_{b,n}\right) &= 1 \qquad \left(x_k \geqq x_{b,n}\right) \end{aligned}\right\} \qquad (D7)$$

By performing the indicated substitutions in equation (D6), integrating, and neglecting the $\dot{\theta}^2$ term, the bending-moment equation reduces to the form

$$M_{b,n} = C_{b,1}\left[\dot{V}_y + \left(V_x - 2\dot{x}_{cg}\right)\dot{\theta} + g\cos\theta\right] + \left(C_{b,2} + C_{b,\ddot{\theta}}\right)\ddot{\theta} + \sum_i \left(C_{b,3i} + C_{b,\ddot{q}_i}\right)\ddot{q}_i(t) + C_{b,\alpha}\left(\alpha + \alpha_w\right) + C_{b,\dot{\theta}}\dot{\theta}$$

$$+ C_{b,\dot{\alpha}}\left(\dot{\alpha} + \dot{\alpha}_w\right) + \sum_i C_{b,q_i} q_i(t) + \sum_i C_{b,\dot{q}_i}\dot{q}_i(t) + \sum_k U\left(x_k - x_{b,n}\right)\left[m_k\left(x_k - x_{b,n}\right)\left(\omega_k^2\lambda_k + 2\xi_k\omega_k\dot{\lambda}_k\right)\right] \qquad (D8)$$

where the coefficients are defined as follows:

Mass coefficients:

$$C_{b,1} = -\int_{x_{b,n}}^{L} \left(x - x_{b,n}\right) m(x,t)\, dx$$

$$C_{b,2} = -\int_{x_{b,n}}^{L} \left(x - x_{b,n}\right)\left(x - x_{cg}\right) m(x,t)\, dx$$

$$C_{b,3i} = -\int_{x_{b,n}}^{L} \left(x - x_{b,n}\right)\phi_i(x)\, m(x,t)\, dx$$

Momentum aerodynamic coefficients:

$$C_{b,\alpha} = \rho S_o\left[-V_{m,w}^2 \int_{x_{b,n}}^{L} \left(x - x_{b,n}\right)\frac{S'(x)}{S_o}\, dx + \dot{V}_{m,w} \int_{x_{b,n}}^{L} \left(x - x_{b,n}\right)\frac{S(x)}{S_o}\, dx\right]$$

$$C_{b,\dot{\theta}} = \rho S_o V_{m,w} \left[\int_{x_{b,n}}^{L} \left(x - x_{b,n}\right)\left(x - x_{cg}\right) \frac{S'(x)}{S_o}\, dx + \int_{x_{b,n}}^{L} \left(x - x_{b,n}\right) \frac{S(x)}{S_o}\, dx \right]$$

$$C_{b,\dot{\alpha}} = \rho S_o V_{m,w} \left[\int_{x_{b,n}}^{L} \left(x - x_{b,n}\right) \frac{S(x)}{S_o}\, dx \right]$$

$$C_{b,\ddot{\theta}} = \rho S_o \left[-\int_{x_{b,n}}^{L} \left(x - x_{b,n}\right)\left(x - x_{cg}\right) \frac{S(x)}{S_o}\, dx \right]$$

$$C_{b,q_i} = \rho S_o \left[-V_{m,w}^2 \int_{x_{b,n}}^{L} \left(x - x_{b,n}\right) \frac{S'(x)}{S_o} \phi_i'(x)\, dx - V_{m,w}^2 \int_{x_{b,n}}^{L} \left(x - x_{b,n}\right) \frac{S(x)}{S_o} \phi_i''(x)\, dx \right.$$

$$\left. + \dot{V}_{m,w} \int_{x_{b,n}}^{L} \left(x - x_{b,n}\right) \frac{S(x)}{S_o} \phi_i'(x)\, dx \right]$$

$$C_{b,\dot{q}_i} = \rho S_o V_{m,w} \left[\int_{x_{b,n}}^{L} \left(x - x_{b,n}\right) \frac{S'(x)}{S_o} \phi_i(x)\, dx + 2 \int_{x_{b,n}}^{L} \left(x - x_{b,n}\right) \frac{S(x)}{S_o} \phi_i'(x)\, dx \right]$$

$$C_{b,\ddot{q}_i} = \rho S_o \left[-\int_{x_{b,n}}^{L} \left(x - x_{b,n}\right) \frac{S(x)}{S_o} \phi_i(x)\, dx \right]$$

Quasi-steady aerodynamic coefficients:

$$C_{b,\alpha} = qS_o \int_{x_{b,n}}^{L} \left(x - x_{b,n}\right) c_{n_\alpha}(x,M)\, dx$$

$$C_{b,\dot{\theta}} = -\frac{qS_o}{V_{m,w}} \int_{x_{b,n}}^{L} \left(x - x_{b,n}\right)\left(x - x_{cg}\right) c_{n_\alpha}(x,M)\, dx$$

$$C_{b,\dot{\alpha}} = 0$$

$$C_{b,\ddot{\theta}} = 0$$

$$C_{b,q_i} = qS_o \int_{x_{b,n}}^{L} \left(x - x_{b,n}\right) \phi_i'(x)\, c_{n_\alpha}(x,M)\, dx$$

$$C_{b,\dot{q}_i} = -\frac{qS_o}{V_{m,w}} \int_{x_{b,n}}^{L} \left(x - x_{b,n}\right) \phi_i(x)\, c_{n_\alpha}(x,M)\, dx$$

$$C_{b,\ddot{q}_i} = 0$$

APPENDIX E

SUMMARY OF EQUATIONS

This appendix summarizes the basic equations. Coefficients are defined in appendixes A, B, and D.

Axial motion equation:

$$m_t\dot{V}_x = m_t\ddot{x}_{cg} + m_tV_y\dot{\theta} + m_e\left[2\dot{\theta}\sum_i \phi_i(0)\,\dot{q}_i(t) + \ddot{\theta}\sum_i \phi_i(0)\,q_i(t)\right] - S_e\left\{2\dot{\theta}\sum_i \phi_i'(0)\,\dot{q}_i(t) + \ddot{\theta}\sum_i \phi_i'(0)\,q_i(t)\right.$$

$$\left. + \sum_i\sum_j \phi_i'(0)\,\phi_j'(0)\left[q_i(t)\,\ddot{q}_j(t) + \dot{q}_i(t)\,\dot{q}_j(t)\right]\right\} + S_{e,l}\left[2\dot{\theta}\dot{\delta} + \ddot{\theta}\delta - \delta\ddot{\delta} - \dot{\delta}^2 + 2\dot{\delta}\sum_i \phi_i'(0)\,\dot{q}_i(t) + \delta\sum_i \phi_i'(0)\,\ddot{q}_i(t)\right.$$

$$\left. + \ddot{\delta}\sum_i \phi_i'(0)\,q_i(t)\right] + \sum_k m_k\left(2\dot{\theta}\dot{\lambda}_k + \ddot{\theta}\lambda_k\right) - m_t\,g\sin\theta - qS_oC_A(M) + T_e$$

Lateral motion equation:

$$m_t\dot{V}_y = -m_t\left(V_x - \dot{x}_{cg}\right)\dot{\theta} - m_e\sum_i \phi_i(0)\,\ddot{q}_i(t) + S_e\sum_i \phi_i'(0)\,\ddot{q}_i(t) - S_{e,l}\ddot{\delta} - \sum_k m_k\ddot{\lambda}_k + \dot{\theta}^2\sum_k m_k\lambda_k - m_tg\cos\theta + C_{n,\alpha}(\alpha + \alpha_w) + C_{n,\dot{\theta}}\dot{\theta}$$

$$+ C_{n,\dot{\alpha}}\left(\dot{\alpha} + \dot{\alpha}_w\right) + C_{n,\ddot{\theta}}\ddot{\theta} + \sum_i C_{n,q_i}q_i(t) + \sum_i C_{n,\dot{q}_i}\dot{q}_i(t) + \sum_i C_{n,\ddot{q}_i}\ddot{q}_i(t) - T_{e,l}\delta + T_e\sum_i \phi_i'(0)\,q_i(t)$$

Pitch equation:

$$\left(I_{cg} + I_e + m_ex_{cg}^2 + 2S_ex_{cg}\right)\ddot{\theta} = -\dot{I}_{cg}\dot{\theta} + m_e\left[\left(\dot{V}_x - \ddot{x}_{cg} + g\sin\theta\right)\sum_i \phi_i(0)\,q_i(t) + x_{cg}\sum_i \phi_i(0)\,\ddot{q}_i(t) - V_y\dot{\theta}\sum_i \phi_i(0)\,q_i(t)\right]$$

$$+ S_e\left[-\left(\dot{V}_x - \ddot{x}_{cg} + g\sin\theta\right)\sum_i \phi_i'(0)\,q_i(t) + \sum_i \phi_i(0)\,\ddot{q}_i(t) - x_{cg}\sum_i \phi_i'(0)\,\ddot{q}_i(t) + V_y\dot{\theta}\sum_i \phi_i'(0)\,q_i(t)\right.$$

$$\left. + V_y\sum_i\sum_j \phi_i'(0)\,\phi_j'(0)\,q_i(t)\,\dot{q}_j(t)\right] + S_{e,l}\left[\left(\dot{V}_x - \ddot{x}_{cg} + g\sin\theta\right)\delta + x_{cg}\ddot{\delta} - V_y\dot{\theta}\delta + V_y\delta\dot{\delta}\right.$$

$$\left. - V_y\delta\sum_i \phi_i'(0)\,\dot{q}_i(t) - V_y\dot{\delta}\sum_i \phi_i'(0)\,q_i(t)\right] + I_e\left[-\sum_i \phi_i'(0)\,\ddot{q}_i(t)\right] + I_{e,l}\ddot{\delta} - \sum_k m_k\left[\ddot{\lambda}_k\left(x_k - x_{cg}\right)\right.$$

$$\left. - \left(\dot{V}_x - \ddot{x}_{cg} + g\sin\theta\right)\lambda_k + V_y\dot{\theta}\lambda_k\right] + C_{m,\alpha}\left(\alpha + \alpha_w\right) + C_{m,\dot{\theta}}\dot{\theta} + C_{m,\dot{\alpha}}\left(\dot{\alpha} + \dot{\alpha}_w\right) + C_{m,\ddot{\theta}}\ddot{\theta} + \sum_i C_{m,q_i}q_i(t)$$

(Equation continued on next page)

$$+ \sum_i C_{m,\dot{q}_i}\dot{q}_i(t) + \sum_i C_{m,\ddot{q}_i}\ddot{q}_i(t) + T_{e,l}x_{cg}\delta - T_e x_{cg}\sum_i \phi_i'(0)\, q_i(t) - T_e \sum_i \phi_i(0)\, q_i(t) - \ddot{\theta}\sum_i m_i q_i^2(t)$$

$$- 2\dot{\theta}\sum_i m_i q_i(t)\,\dot{q}_i(t) - \dot{\theta}\sum_i \dot{m}_i q_i^2(t) - \ddot{\theta}\sum_k m_k\lambda_k^2 - 2\dot{\theta}\sum_k m_k\lambda_k\dot{\lambda}_k - 2\ddot{\theta}\sum_k\sum_i m_k\lambda_k\phi_i(x_k)\, q_i(t)$$

$$- 2\dot{\theta}\sum_k\sum_i m_k\dot{\lambda}_k\phi_i(x_k)\, q_i(t) - 2\dot{\theta}\sum_k\sum_i m_k\lambda_k\phi_i(x_k)\,\dot{q}_i(t) - m_t V_y\dot{x}_{cg} - 2\dot{x}_{cg}\dot{\theta}\left(m_e x_{cg} + S_e\right)$$

jth bending mode equation:

$$m_j\ddot{q}_j(t) = -2m_j\xi_j\omega_j\dot{q}_j(t) - m_j\omega_j^2 q_j(t) - \dot{m}_j\dot{q}_j(t) + m_j q_j(t)\dot{\theta}^2 + m_e\Big[-\dot{V}_y\phi_j(0) + x_{cg}\ddot{\theta}\phi_j(0) - \phi_j(0)\sum_i \phi_i(0)\,\ddot{q}_i(t) - \left(V_x - 2\dot{x}_{cg}\right)\dot{\theta}\phi_j(0)$$

$$- g\phi_j(0)\cos\theta\Big] + S_e\Big[-\left(\dot{V}_x - \ddot{x}_{cg}\right)\phi_j'(0)\sum_i \phi_i'(0)\, q_i(t) + \ddot{\theta}\phi_j(0) + \phi_j(0)\sum_i \phi_i'(0)\,\ddot{q}_i(t) + \phi_j'(0)\dot{V}_y - x_{cg}\phi_j'(0)\ddot{\theta}$$

$$+ \phi_j'(0)\sum_i \phi_i(0)\,\ddot{q}_i(t) + \left(V_x - 2\dot{x}_{cg}\right)\phi_j'(0)\dot{\theta} + g\phi_j'(0)\cos\theta\Big] + S_{e,l}\Big[\left(\dot{V}_x - \ddot{x}_{cg}\right)\phi_j'(0)\delta - \phi_j(0)\ddot{\delta}\Big] + I_e\Big[-\phi_j'(0)\ddot{\theta}$$

$$- \phi_j'(0)\sum_i \phi_i'(0)\,\ddot{q}_i(t)\Big] + I_{e,l}\Big[\phi_j'(0)\ddot{\delta}\Big] - \sum_k m_k\phi_j(x_k)\ddot{\lambda}_k + \dot{\theta}^2\sum_k m_k\lambda_k\phi_j(x_k) + C_{j,\alpha}(\alpha + \alpha_w) + C_{j,\dot{\theta}}\dot{\theta} + C_{j,\dot{\alpha}}\left(\dot{\alpha} + \dot{\alpha}_w\right)$$

$$+ C_{j,\ddot{\theta}}\ddot{\theta} + \sum_i C_{j,q_i}q_i(t) + \sum_i C_{j,\dot{q}_i}\dot{q}_i(t) + \sum_i C_{j,\ddot{q}_i}\ddot{q}_i(t) - T_{e,l}\phi_j(0)\delta + T_e\phi_j(0)\sum_i \phi_i'(0)\, q_i(t)$$

Gimbal engine equations:

$$\ddot{\delta} + 2\xi_{e,l}\omega_{e,l}\dot{\delta} + \omega_{e,l}^2\delta = K_c\omega_e^2\int_0^t(\delta_c - \delta)\,dt + \frac{T_l}{I_{e,l}} + \frac{K_o}{I_{e,l}}\int_0^t T_l\,dt$$

$$T_l = I_{e,l}\sum_i \phi_i'(0)\,\ddot{q}_i(t) - S_{e,l}\left(\dot{V}_x - \ddot{x}_{cg}\right)\delta + S_{e,l}\left(\dot{V}_x - \ddot{x}_{cg}\right)\sum_i \phi_i'(0)\, q_i(t) - S_{e,l}\dot{V}_y + S_{e,l}\ddot{\theta}x_{cg}$$

$$+ I_{e,l}\ddot{\theta} - S_{e,l}\sum_i \phi_i(0)\,\ddot{q}_i(t) - S_{e,l}\left(V_x - 2\dot{x}_{cg}\right)\dot{\theta} - S_{e,l}g\cos\theta$$

Propellant slosh equation:

$$\ddot{\lambda}_k + 2\xi_k\omega_k\dot{\lambda}_k + \omega_k^2\lambda_k = -\dot{V}_y - \left(x_k - x_{cg}\right)\ddot{\theta} - \sum_i \phi_i\left(x_k\right)\ddot{q}_i(t) - \left(V_x - 2\dot{x}_{cg}\right)\dot{\theta}$$

$$+ \lambda_k\dot{\theta}^2 + \dot{\theta}^2\sum_i \phi_i\left(x_k\right)\, q_i(t) - g\cos\theta$$

Control system equations:

$$\ddot{\delta}_c + 2\xi_f\omega_f\dot{\delta}_c + \omega_f^2\delta_c = a_o\left[K_f\dot{\theta}_e + \omega_f\left(\omega_f + 2K_f\xi_f\right)\theta_e + K_f\omega_f^2\int_0^t \theta_e\, dt\right]$$

$$\theta_e = \theta_c - \theta_f$$

$$\theta_f = \theta + \sum_i \phi_i'(x_\theta)\, q_i(t) + \mu_1\left[\dot{\theta} + \sum_i \phi_i'(x_{\dot{\theta}})\, \dot{q}_i(t)\right] + \mu_2\alpha_s$$

$$\alpha_s = \alpha + \alpha_w + \sum_i \phi_i'(x_\alpha)\, q_i(t) - \frac{1}{V_{m,w}}\left[(x_\alpha - x_{cg})\dot{\theta} + \sum_i \phi_i(x_\alpha)\, \dot{q}_i(t)\right]$$

Bending-moment equations:

$$M_{b,n} = C_{b,1}\left[\dot{V}_y + \left(V_x - 2\dot{x}_{cg}\right)\dot{\theta} + g\cos\theta\right] + \left(C_{b,2} + C_{b,\ddot{\theta}}\right)\ddot{\theta} + \sum_i \left(C_{b,3i} + C_{b,\ddot{q}_i}\right)\ddot{q}_i(t) + C_{b,\alpha}\left(\alpha + \alpha_w\right) + C_{b,\dot{\theta}}\dot{\theta}$$

$$+ C_{b,\dot{\alpha}}\left(\dot{\alpha} + \dot{\alpha}_w\right) + \sum_i C_{b,q_i}q_i(t) + \sum_i C_{b,\dot{q}_i}\dot{q}_i(t) + \sum_k U\left(x_k - x_{b,n}\right)\left[m_k\left(x_k - x_{b,n}\right)\left(\omega_k^2\lambda_k + 2\xi_k\omega_k\dot{\lambda}_k\right)\right]$$

$$U\left(x_k - x_{b,n}\right) = 0 \qquad \left(x_k < x_{b,n}\right)$$

$$U\left(x_k - x_{b,n}\right) = 1 \qquad \left(x_k \geqq x_{b,n}\right)$$

Miscellaneous equations:

$$V_{m,w} = \sqrt{V_m^2 + V_w^2 + 2V_mV_w\cos\gamma}$$

$$V_m = \sqrt{V_x^2 + V_y^2}$$

$$\alpha_w = \sin^{-1}\left(\frac{V_w\sin\gamma}{V_{m,w}}\right)$$

$$\alpha = \tan^{-1}\left(\frac{-V_y}{V_x}\right)$$

$$\gamma = \theta - \alpha$$

$$h(t) = \int_0^t V_m \sin \gamma \, dt$$

$$r(t) = \int_0^t V_m \cos \gamma \, dt$$

$$q = \frac{1}{2}\rho V_{m,w}^2$$

$$\dot{m}_t = w_1 + w_2$$

$$T_{e,1} = T_{v,1} - A_1 p_o$$

$$T_e = T_v - \left(A_1 + A_2\right)p_o$$

$$T_{v,1} = -w_1 V_1 + A_1 p_{e,1}$$

$$T_v = T_{v,1} - w_2 V_2 + A_2 p_{e,2}$$

$$\omega_k = \sqrt{\Omega_k a_x}$$

$$M = \frac{V_{m,w}}{V_s}$$

REFERENCES

1. Lukens, David R., Schmitt, Alfred F., and Broucek, George T.: Approximate Transfer Functions for Flexible-Booster-and-Autopilot Analysis. WADD TR-61-93, U.S. Air Force, Apr. 1961.

2. Mazzola, Luciano L.: Design Criteria for Wind-Induced Flight Loads on Large Boosted Vehicles. AIAA Jour. (Tech. Notes and Comments), vol. 1, no. 4, Apr. 1963, pp. 913-914.

3. Hobbs, Norman P., Criscione, Emanuel S., Mazzola, Luciano L., and Frassinelli, Guido J.: Development of Interim Wind, Wind Shear, and Gust Design Criteria for Vertically-Rising Vehicles. WADC Tech. Rep. 59-504, U.S. Air Force, July 1959.

4. Sissenwine, Norman: Development of Missile Design Wind Profiles for Patrick AFB. Air Force Surveys in Geophysics No. 96 (AFCRC-TN-58-216, ASTIA Doc. No. AD.146870), Air Force Cambridge Res. Center, Mar. 1958.

5. Kachigan, K.: The General Theory and Analysis of a Flexible Bodied Missile With Autopilot Control. Rep. ZU-7-048 (Contract No. AF04(645)-4), CONVAIR, Nov. 11, 1955.

6. Henry, Robert M., Brandon, George W., Tolefson, Harold B., and Lanford, Wade E.: The Smoke-Trail Method for Obtaining Detailed Measurements of the Vertical Wind Profile for Application to Missile-Dynamic-Response Problems. NASA TN D-976, 1961.

7. Edelen, Dominic G. B.: On the Dynamical Effects of Fuel Flow on the Motion of Boost Vehicles. Memo. RM-3268-NASA (Contract No. NASr-21(03)), The RAND Corp., Oct. 1962.

8. Bisplinghoff, Raymond L., Ashley, Holt, and Halfman, Robert L.: Aeroelasticity. Addison-Wesley Pub. Co., Inc. (Cambridge, Mass.), c.1955.

9. Houbolt, John C., and Anderson, Roger A.: Calculation of Uncoupled Modes and Frequencies in Bending or Torsion of Nonuniform Beams. NACA TN 1522, 1948.

10. Young, Dana: Generalized Missile Dynamics Analysis. II - Equations of Motion. GM-TR-0165-00359, Space Tech. Labs., The Ramo-Wooldridge Corp., Apr. 7, 1958.

11. Bauer, Helmut F.: Theory of the Fluid Oscillations in a Circular Cylindrical Ring Tank Partially Filled With Liquid. NASA TN D-557, 1960.

12. Lukens, David R.: Methods of Analysis of a Control System for a Large Flexible Missile. Proc. Nat. Specialists Meeting on Guidance of Aerospace Vehicles (Boston, Mass.), Inst. Aero. Sci., May 1960, pp. 98-107.

13. Stephens, David G., Leonard, H. Wayne, and Perry, Tom W., Jr.: Investigation of the Damping of Liquids in Right-Circular Cylindrical Tanks, Including the Effects of a Time-Variant Liquid Depth. NASA TN D-1367, 1962.

14. Silveira, Milton A., Stephens, David G., and Leonard, H. Wayne: An Experimental Investigation of the Damping of Liquid Oscillations in Cylindrical Tanks With Various Baffles. NASA TN D-715, 1961.

15. Whittaker, E. T.: A Treatise on the Analytical Dynamics of Particles and Rigid Bodies. Fourth ed., Dover Publications (New York), 1944.

16. Corben, H. C., and Stehle, Philip: Classical Mechanics. 2nd ed., John Wiley & Sons, Inc., c.1960.

17. Thomson, William Tyrrell: Introduction to Space Dynamics. John Wiley & Sons, Inc., c.1961.

18. Scanlan, Robert H., and Rosenbaum, Robert: Introduction to the Study of Aircraft Vibration and Flutter. The Macmillan Co., 1951.

19. Miles, J. W., and Young, Dana: Generalized Missile Dynamics Analysis. III - Aerodynamics. GM-TR-0165-00360, Space Tech. Labs., The Ramo-Wooldridge Corp., Apr. 7, 1958.

20. Backus, F. I.: Describing Functions for Nonlinear Electrohydraulic Gimbaled Rocket-Engine Position Servos With Application to Closed-Loop Control Systems. Rep. No. AE60-0287 (Contract No. AF 04(647)-299), Convair-Astronautics, June 10, 1960.

21. Anon.: U.S. Standard Atmosphere, 1962. NASA, U.S. Air Force, and Weather Bureau, Dec. 1962.

22. Hartree, D. R.: Numerical Analysis. Second ed., The Clarendon Press (Oxford), 1958.

23. Henrici, Peter: Discrete Variable Methods in Ordinary Differential Equations. John Wiley & Sons, Inc., c.1962.

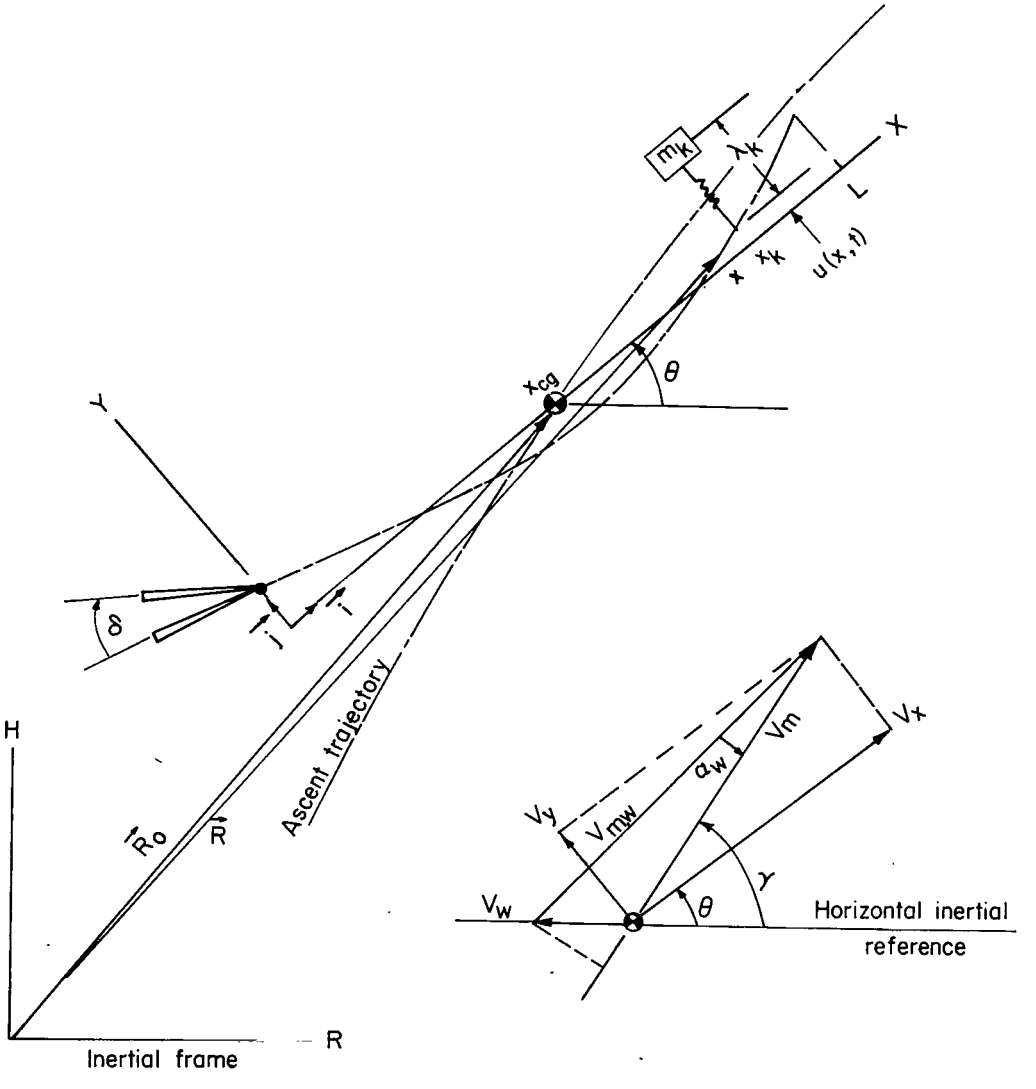

Figure 1.- Coordinate system.

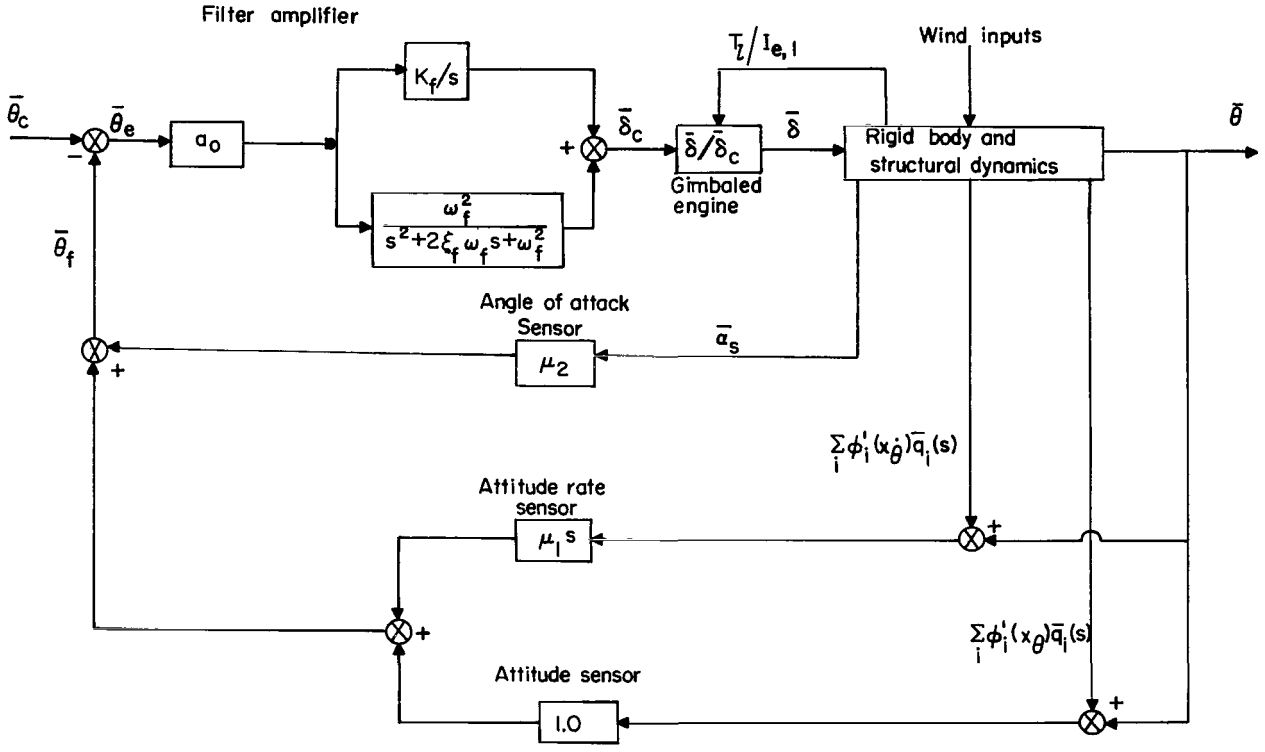

Figure 2.- System block diagram.

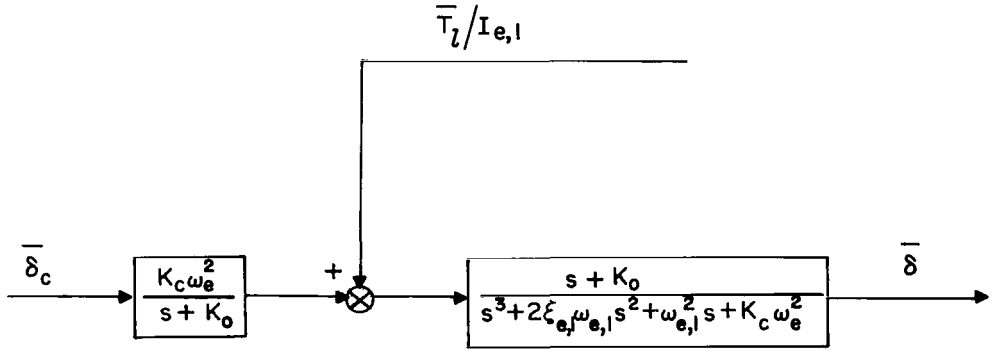

Figure 3.- Gimbaled engine block diagram.

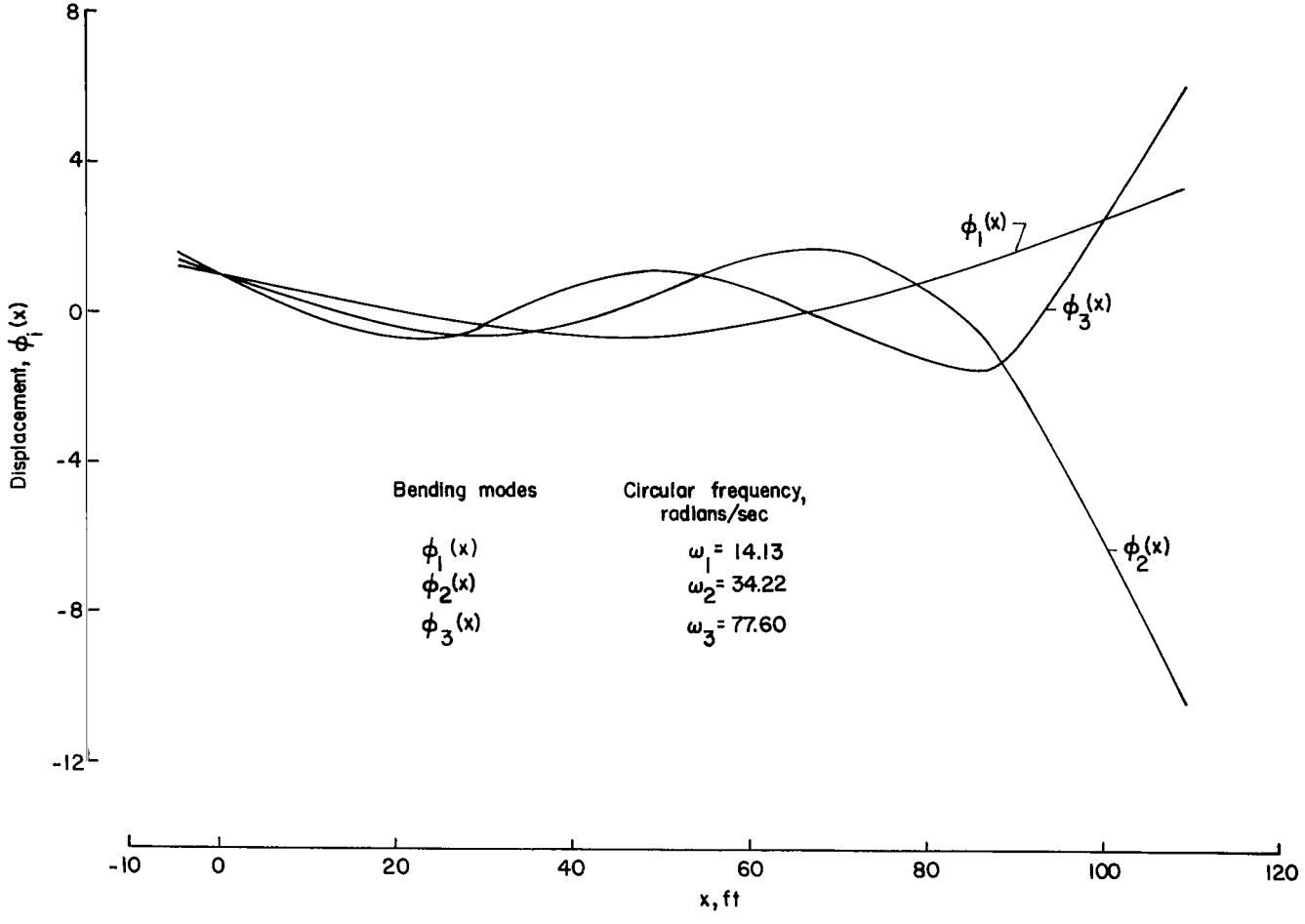

Figure 4.- Bending modes. t = 62 sec.

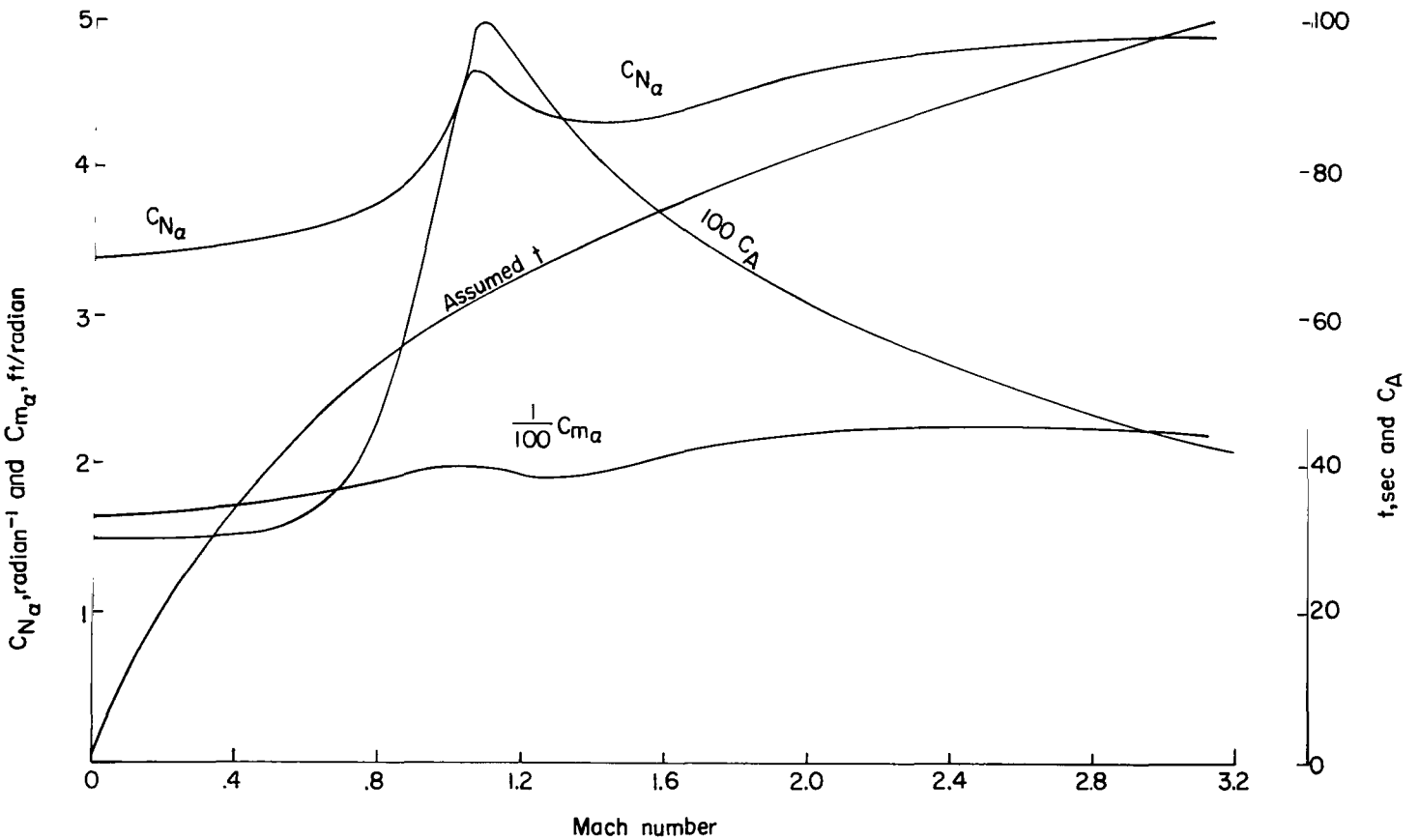

Figure 5.- Aerodynamic data.

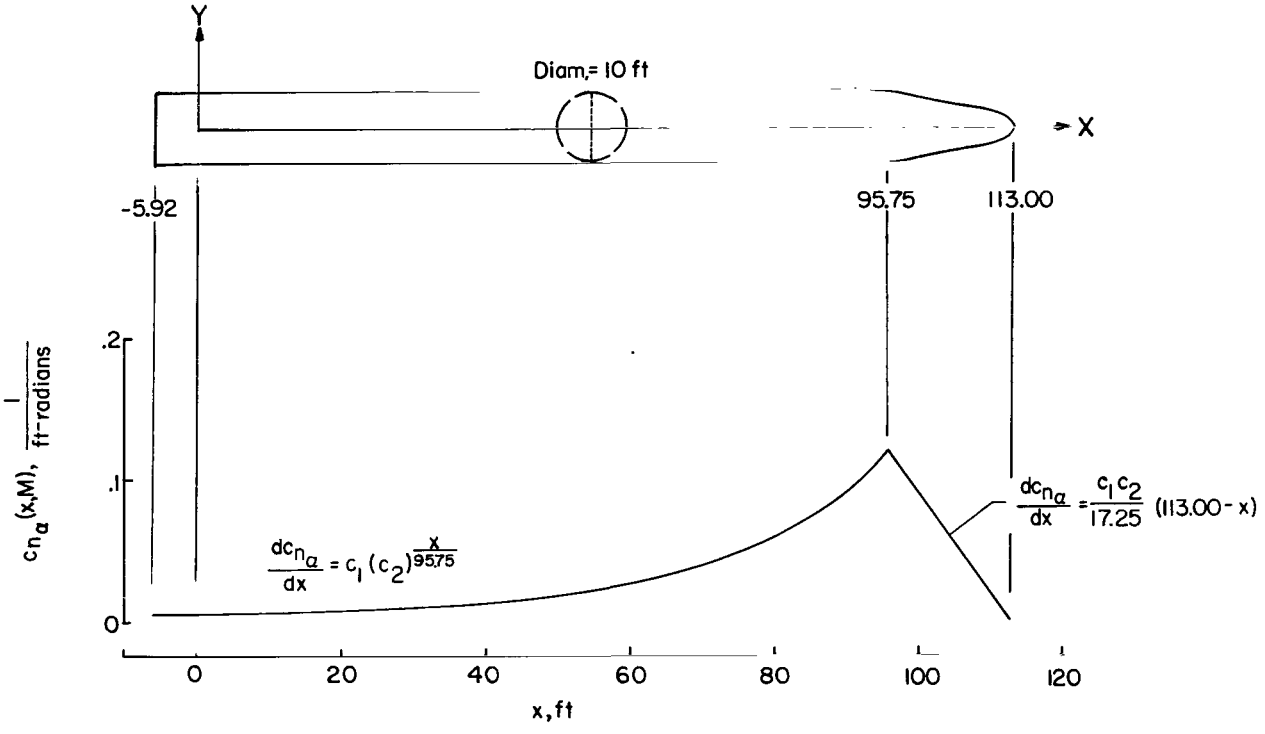

Figure 6.- Example launch vehicle showing assumed normal-force distribution. M = 2.0.

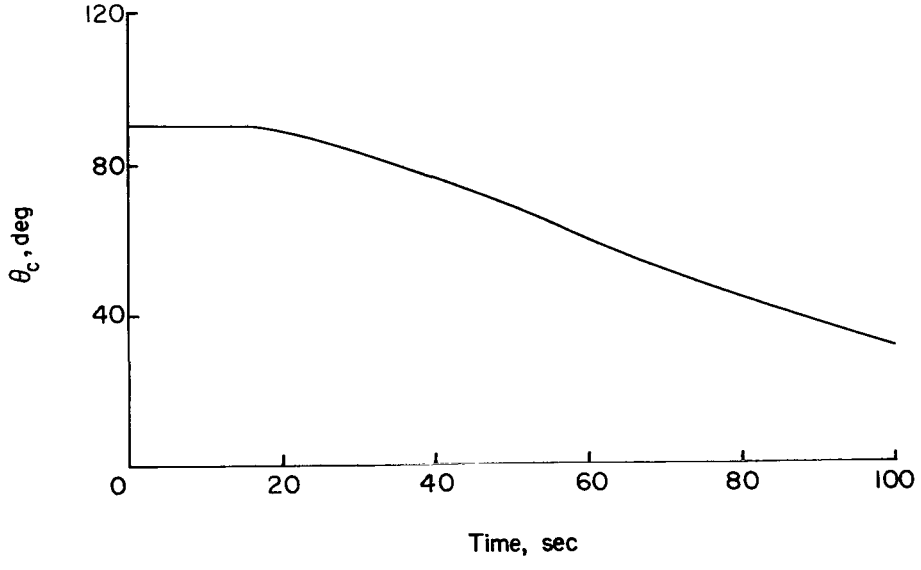

Figure 7.- Pitch program.

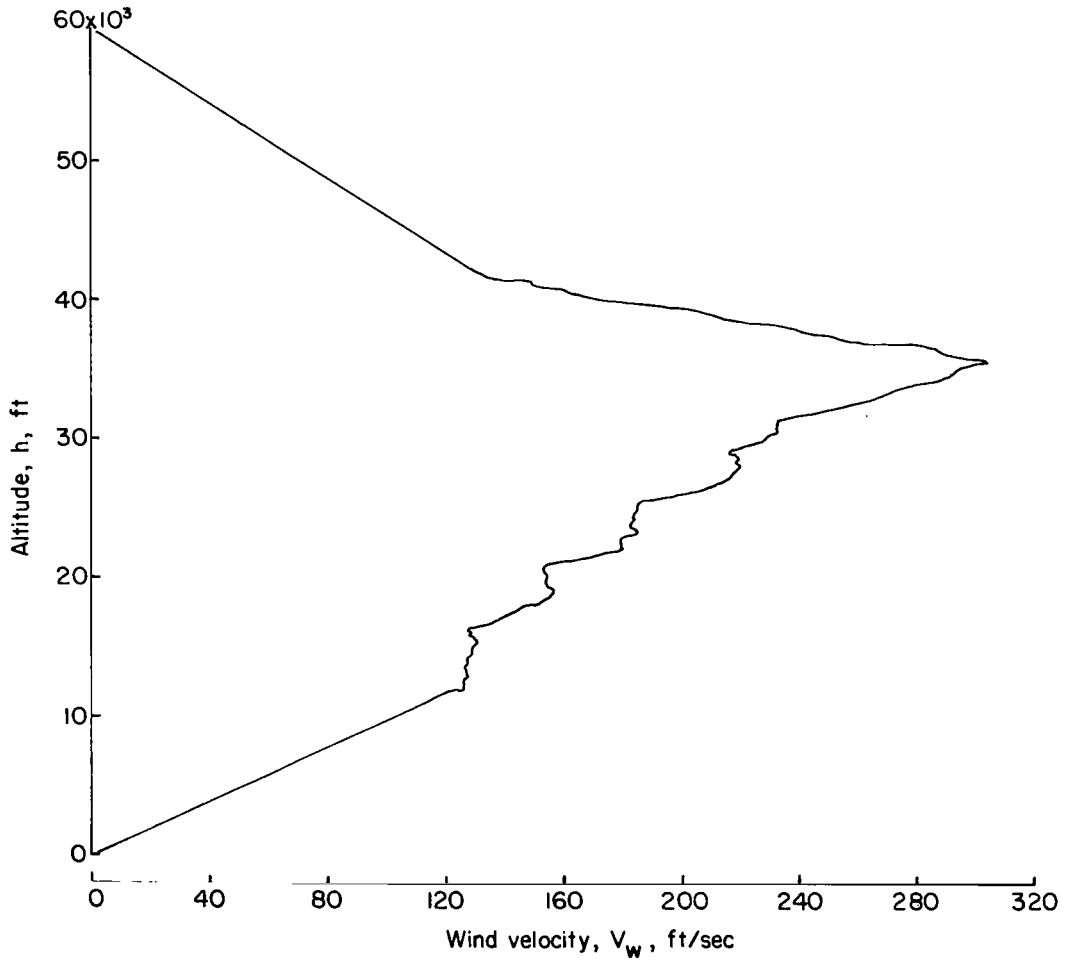

Figure 8.- Wind profile (tailwind).

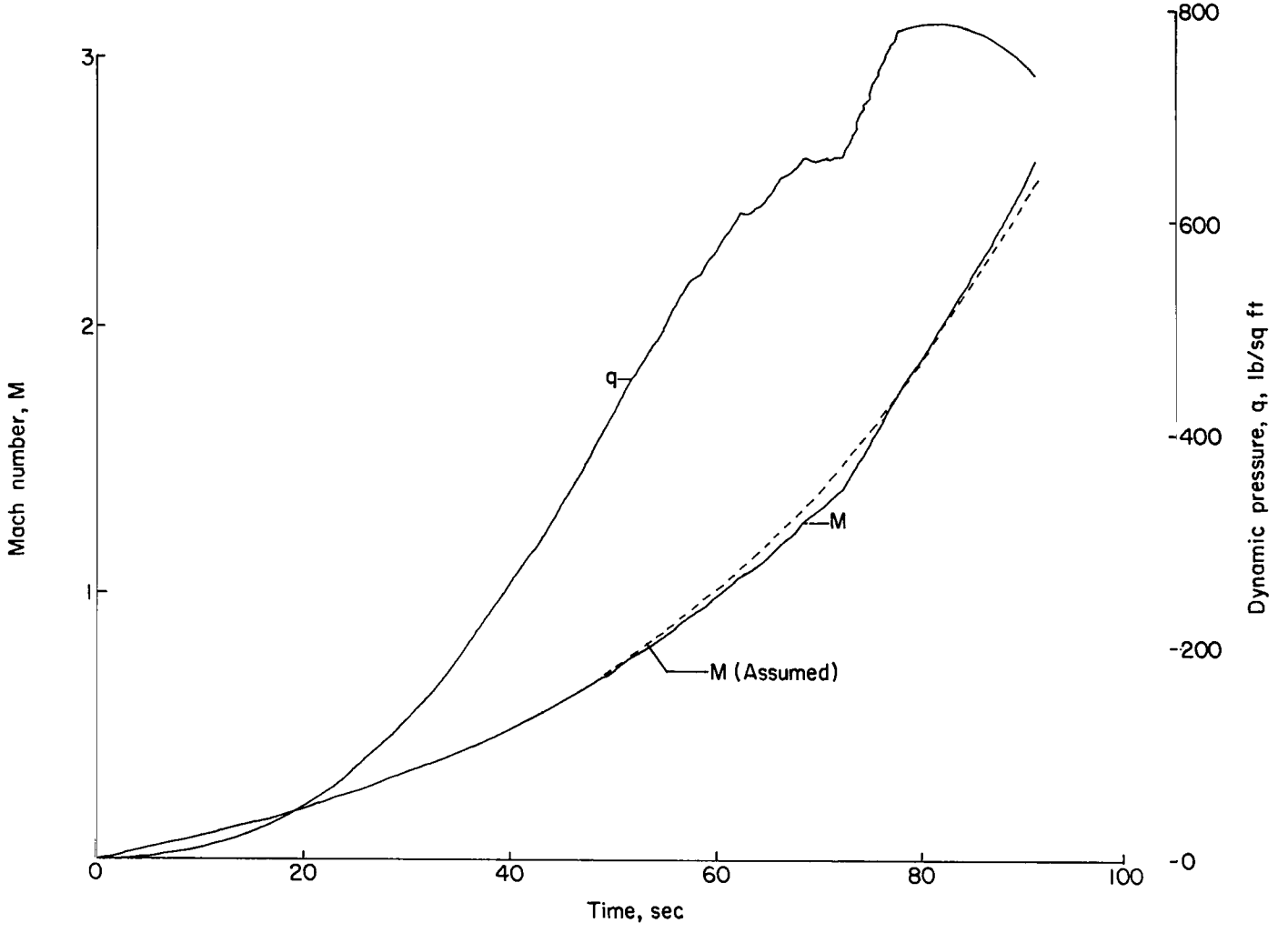

(a) Mach number and dynamic pressure.

Figure 9.- Trajectory data.

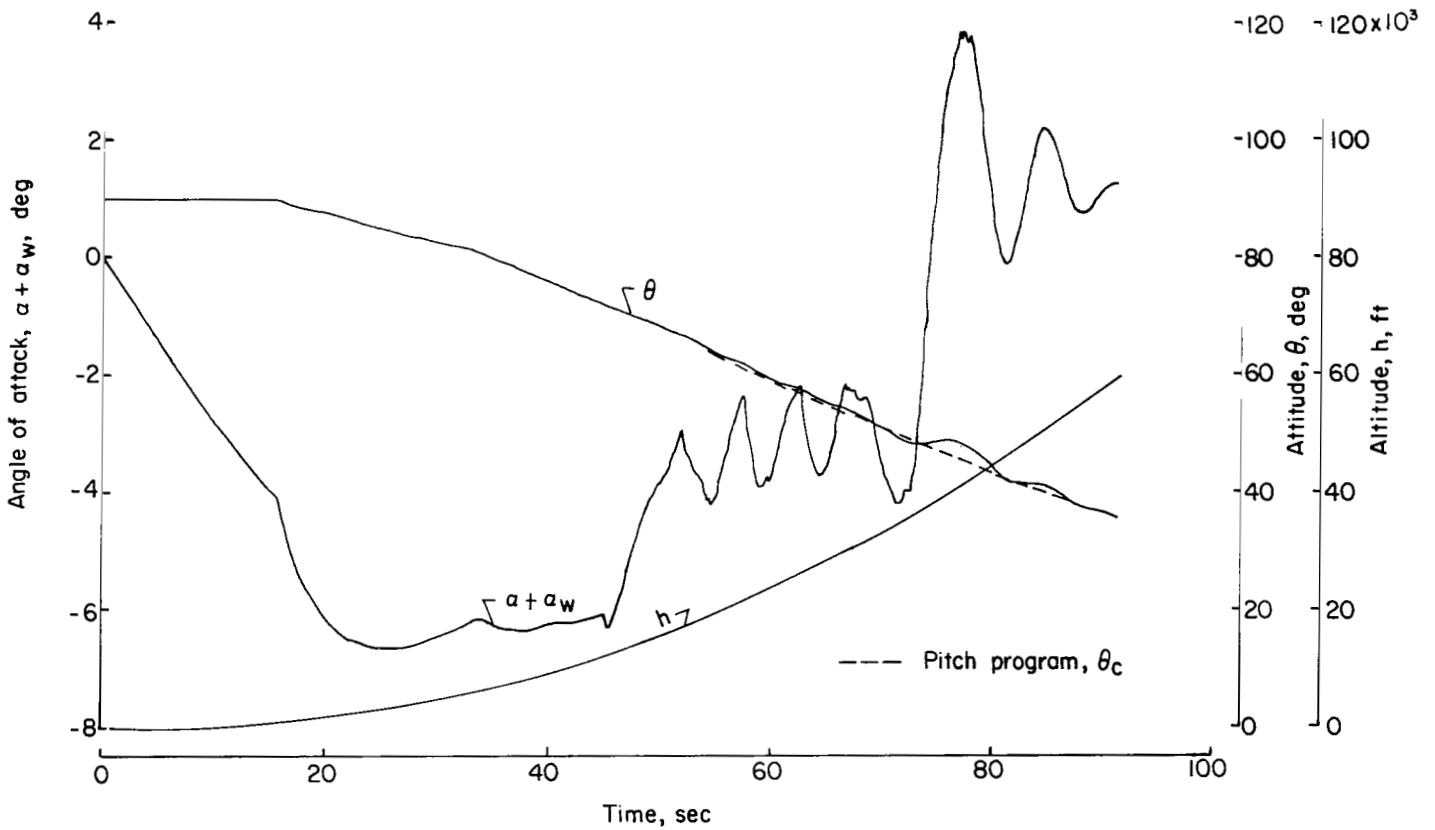

(b) Angle of attack, altitude, and pitch attitude.

Figure 9.- Concluded.

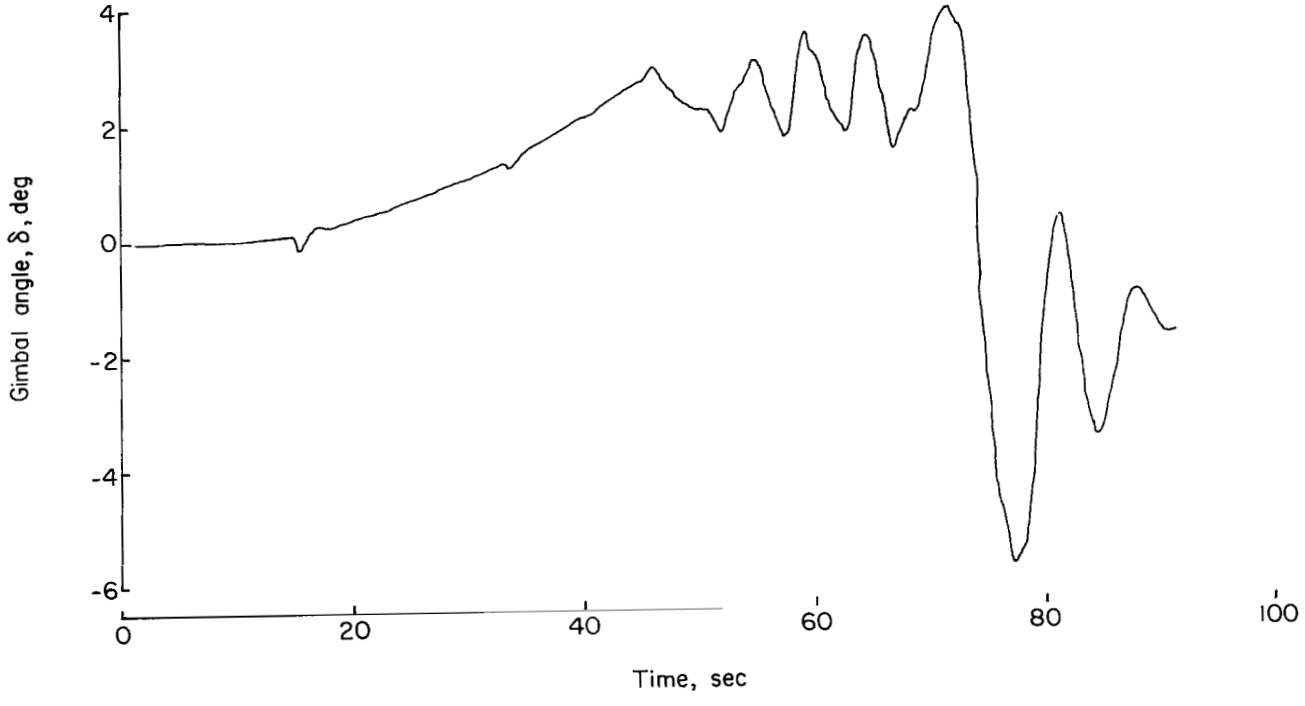

Figure 10.- Gimbaled engine response.

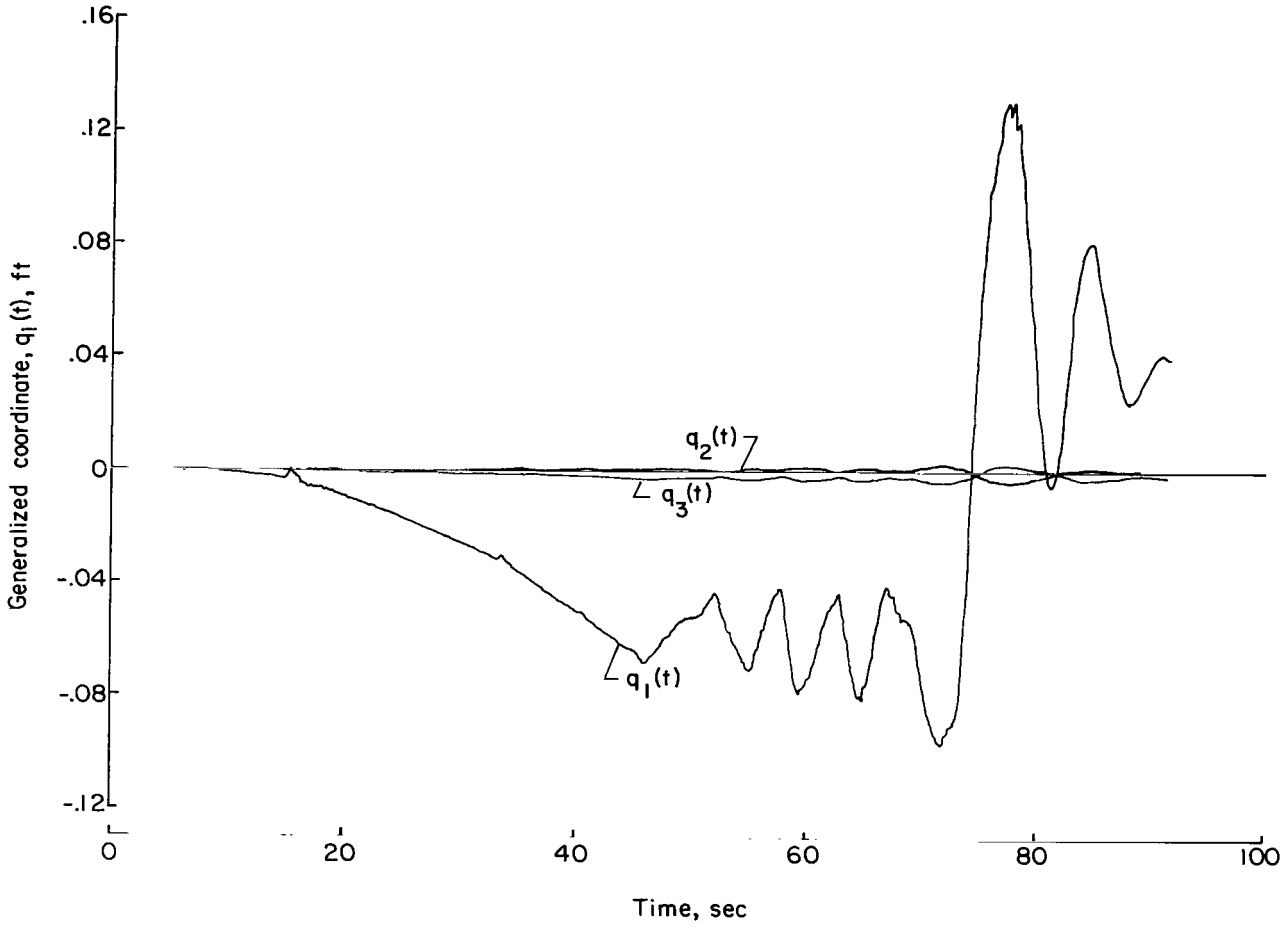

Figure 11.- Bending-mode response.

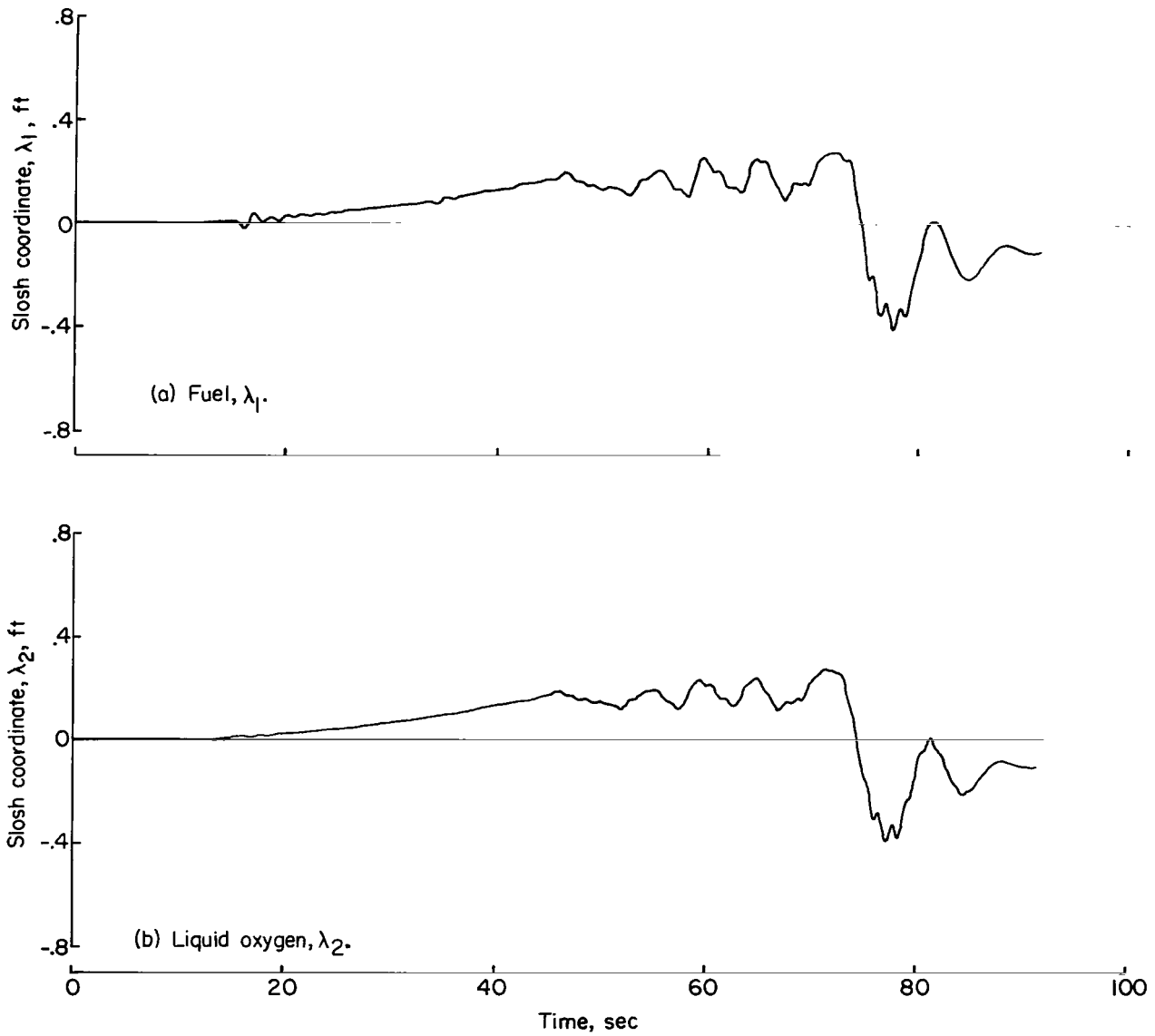

Figure 12.- Propellant slosh response.

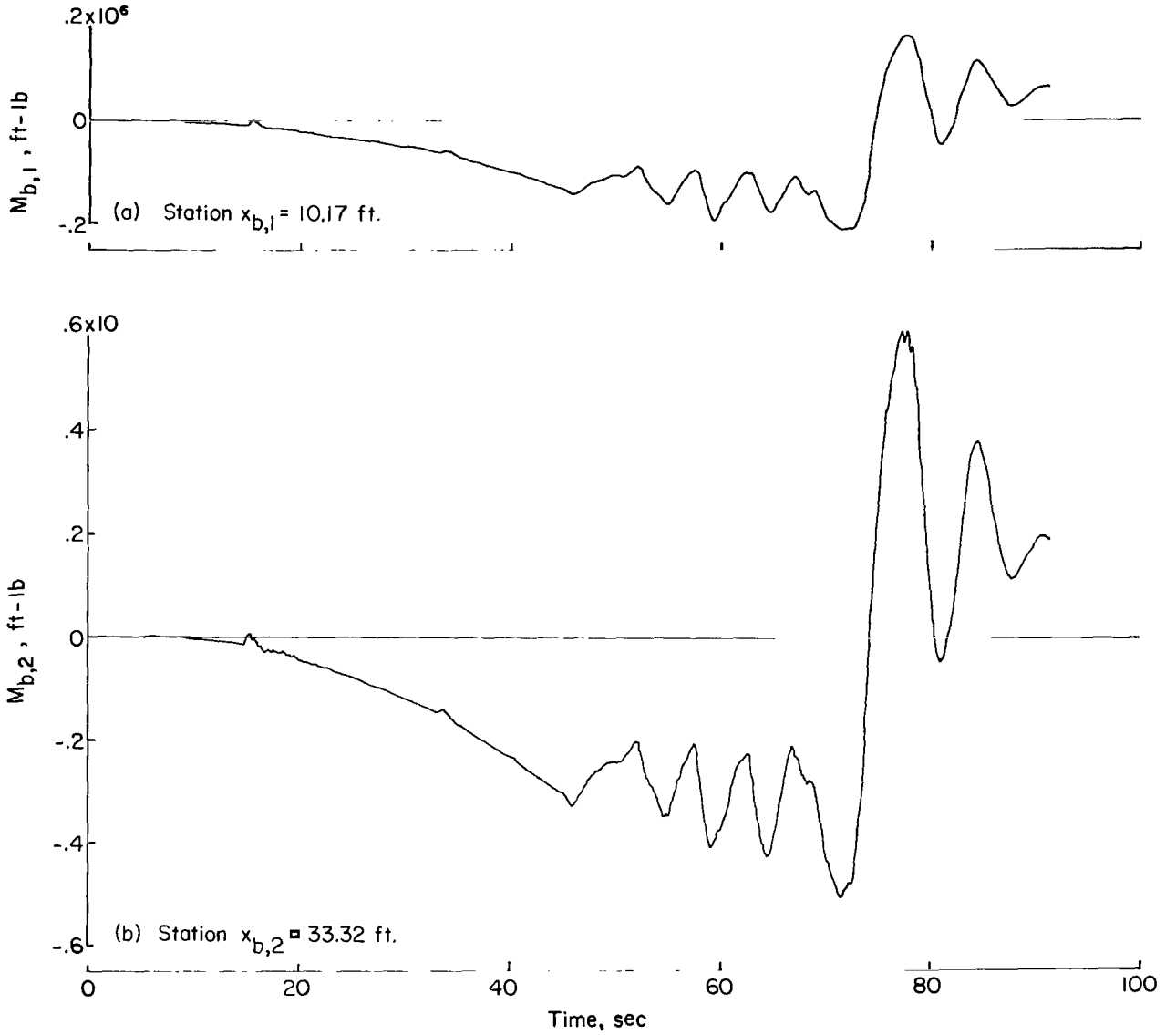

Figure 13.- Bending-moment response.

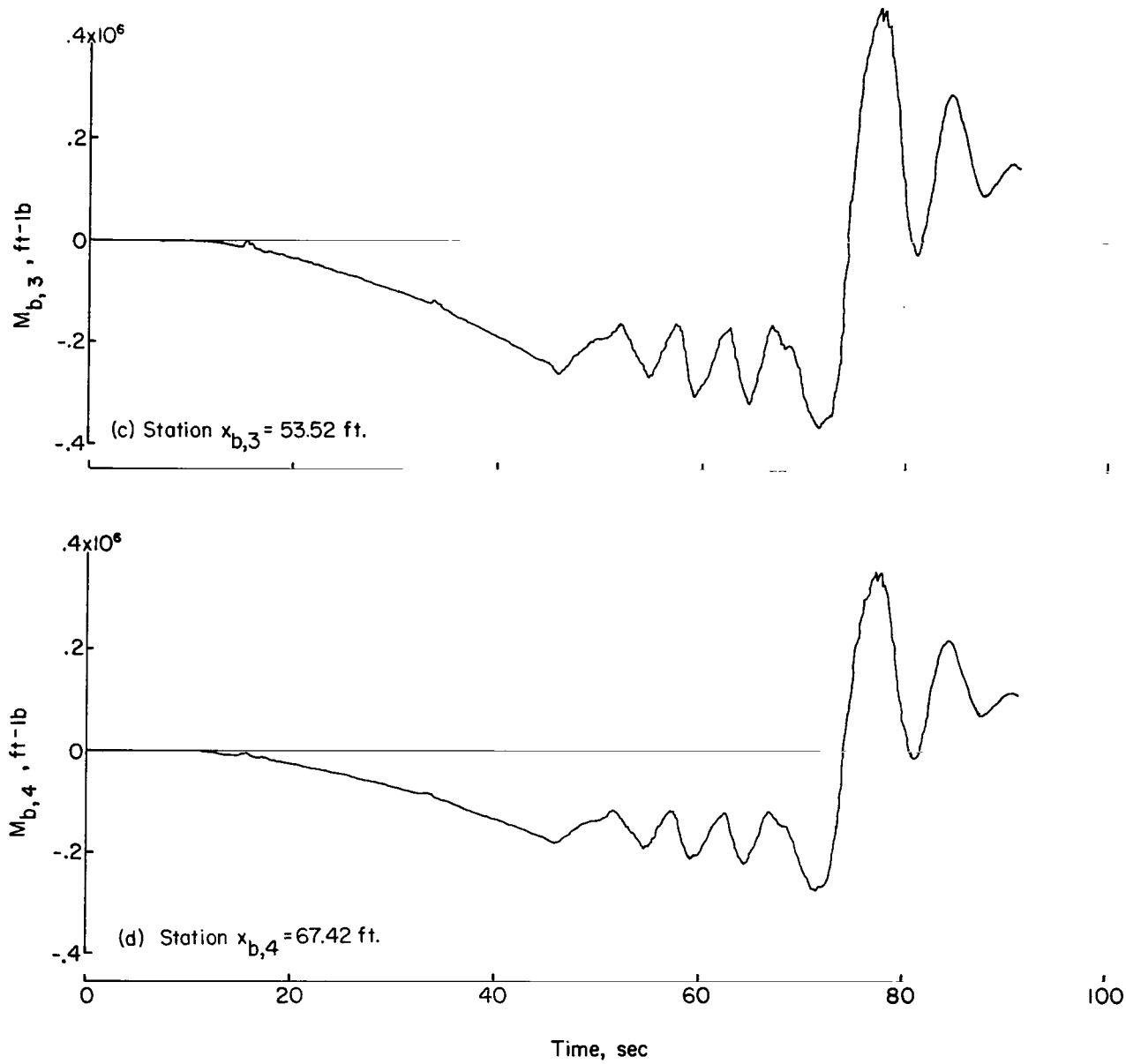

Figure 13.- Continued.

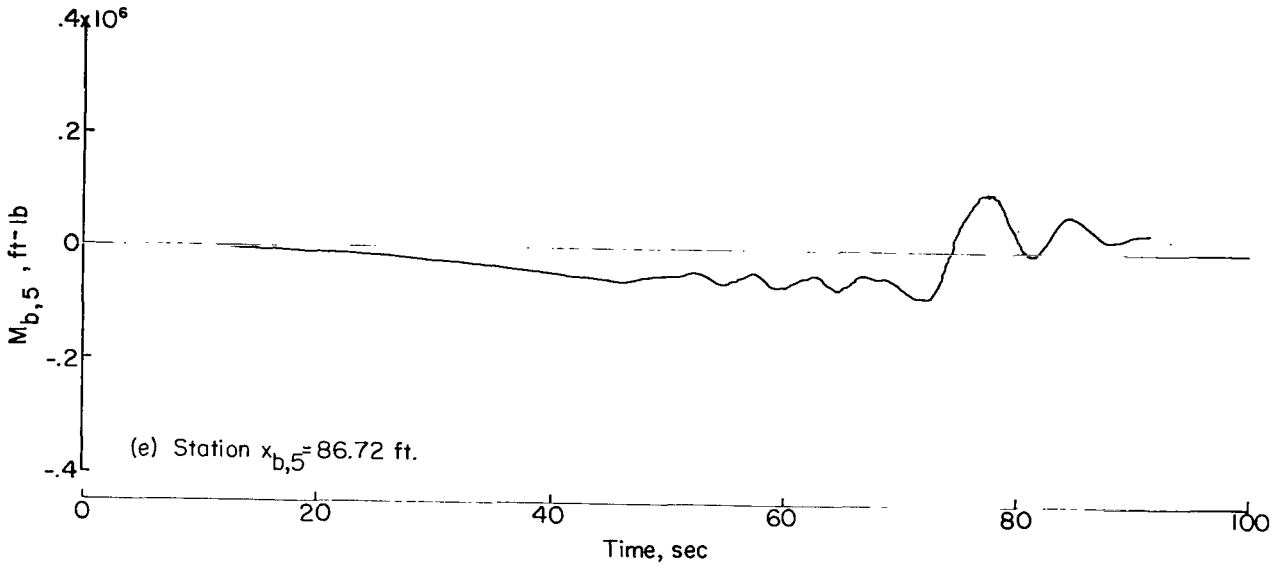

Figure 13.- Concluded.

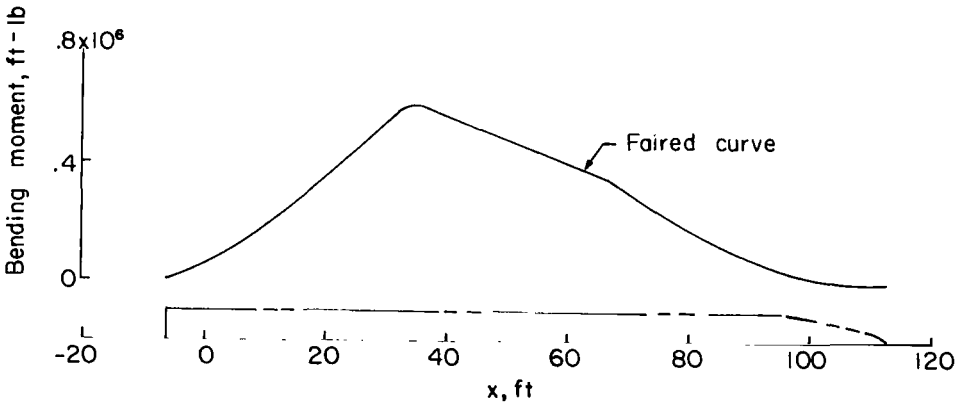

Figure 14.- Bending-moment distribution at t = 77.5 sec.